particularly when neurologic deficits are involved [9]. However, most patients with osteoporotic vertebral compression fractures are elderly and many cases involve serious complications. Therefore, we speculated whether a particularly invasive surgery is unsuitable for them. Furthermore, decompression of the injured spinal cord by laminectomy alone is reported to be insufficient to ameliorate neurologic symptoms [4, 10]. Percutaneous vertebroplasty has been widely used in the world as a treatment method that can be performed less invasively for osteoporotic vertebral compression fractures [11–13] and has been reported to be effective for vertebral pseudarthrosis with serious pain [14, 15]. However, the effectiveness of vertebroplasty for delayed-onset paraplegia has not been elucidated. For vertebral pseudarthrosis with motional cleft, instability was believed to be the major characteristic. Therefore, we hypothesized that stabilizing the body of vertebra by vertebroplasty may contribute to improving motor paralysis due to the vertebral pseudarthrosis.

We performed vertebroplasty for patients with delayed-onset paraplegia due to vertebral pseudarthrosis and tested its effectiveness by evaluating the improvements in neurologic symptoms, the levels of low back pain, the degrees of spinal kyphotic angle and the stabilities of the concerned vertebra.

Materials and methods

Operative technique

Surgery was performed with the patient in a prone position under fluoroscopy, and pads were placed in the thoracic and the pelvic regions to sufficiently open the intravertebral cleft. The surgery was performed under general anaesthesia and checked by an anaesthesiologist during the operation to avoid severe complications due to polymethylmethacrylate (PMMA) [16]. Eight-gauge Jamshidi® needles (Cardinal Health, Inc., Dublin, OH, USA) and a cement gun were used. PMMA (Depuy International, Ltd., Leeds, UK) was refrigerated from the day before the surgery (4°C) to facilitate smooth injection through a bone biopsy needle. The procedure involved two bone marrow biopsy needles that were manually inserted into the bilateral pedicle. Following insertion, a saline solution was injected into the interior of the cleft and sufficient communication between the needles was verified by the flow of the saline solution from the biopsy needle on one side to that on the other side. Subsequently, contrast medium was injected through one biopsy needle and the interior of the cleft was enhanced under fluoroscopy. We ensured that contrast media did not leak out to the intraspinal area or the retroperitoneum in the frontal or lateral view of the fluoroscopy. A cement gun was then used to inject PMMA through a disposable syringe into the interior of the cleft until it leaked from the biopsy needle on the other side (Fig. 1).

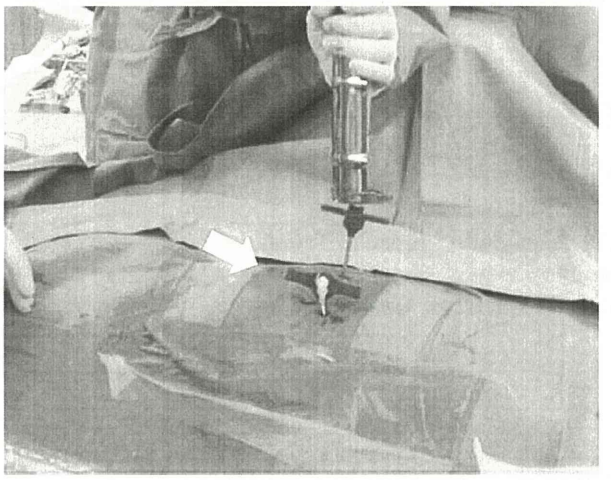

Fig. 1 Photograph shows that the cleft was filled with PMMA until it leaked from the biopsy needle on the other side

Patients and methods

Percutaneous vertebroplasty without spreading the spinal canal was performed on 31 vertebrae in 29 patients all with pseudarthrosis following vertebral compression fractures at our institution from January 2001 to December 2008; 11 vertebrae in 11 of these patients showed delayed-onset motor weakness. The Institutional Review Board of Saitama Medical University approved this study and written informed consent was obtained from all patients. The patients were 3 males and 8 females aged 60–78 years (mean 71.9 ± 5.2 years). The mean follow-up period was 37.2 ± 27.1 months (range 6–95 months). The affected vertebral levels were located in the thoracolumbar junction in all patients with T11 in 2 cases, T12 in 3 and L1 in 6. The period between the onset of motor weakness and the day of the surgery ranged from 3 to 20 weeks with a mean period of 9.5 ± 5.7 weeks (Table 1). All cases had back pain and showed vacuum clefts at the affected vertebrae in lateral supine X-ray views. Only one case required a catheter because of bladder dysfunction (case 3).

Clinical appearance

The back pain was evaluated before and after the surgery using the Denis pain scale (P 1–5) [17]: P 1, no pain; P 2,

Table 1 Summary of patients' data

Case number	Age (years)	Gender	Level of affected vertebra	Period (weeks)	Denis pain scale	Performance status	Weakest muscle groups	MMT	Follow-up period (months)
1	68	F	L1	20	4	3	H/E, H/F	1	95
2	76	F	L1	4	4	2	A/E, H/E	1	9
3	74	F	L1	3	5	4	H/E, H/F	1	71
4	60	M	L1	16	4	3	H/E, H/F	0	48
5	75	F	T12	12	4	2	H/E	2	43
6	69	F	T12	12	4	2	A/E, H/E	1	41
7	74	F	T12	10	5	4	A/E, A/F, H/E, H/F	0	32
8	70	F	T11	10	5	4	K/E, H/E	3	30
9	78	M	T11	3	4	2	H/E	2	21
10	70	M	L1	3	5	4	Hi/F, K/E, A/E, A/F, H/E, H/F	3	6
11	77	F	L1	11	5	4	H/E	1	13
Mean ± SD	71.9 ± 5.2			9.5 ± 5.7					37.2 ± 27.1

Hi/F hip flexors, *K/E* knee extensors, *A/E* ankle extensors, *A/F* ankle flexsors, *H/E* hallucis longus extensor, *H/F* hallucis longus flexor, *MMT* manual muscle testing using the modified Medical Research Council's 0–5 grade, *Period (weeks)* period from the onset of motor weakness until the day of surgery

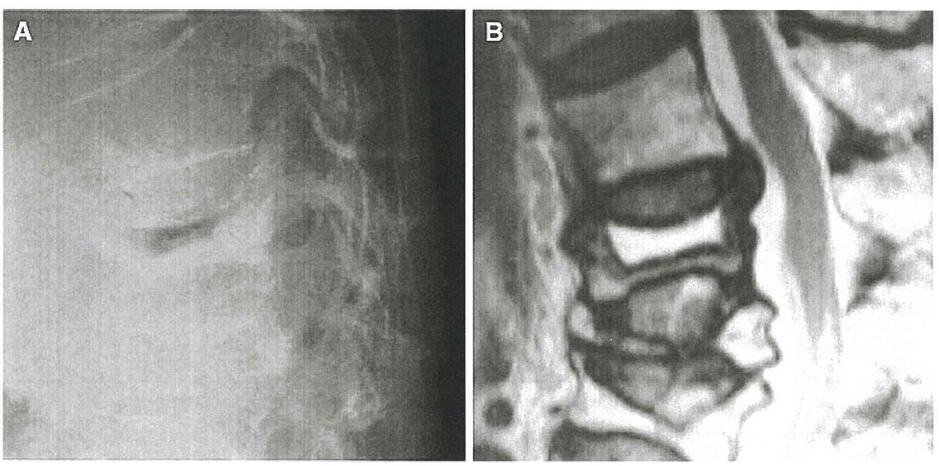

Fig. 2 Lateral X-ray image in supine position shows the cleft in the T12 body (**a**). The sagittal T2-weighted MR image demonstrates a well-defined hyperintensity area marking the intravertebral cleft (**b**)

occasional, minimal pain with no medication required; P 3, moderate pain with occasional medication but no interruption of work or significant changes in activities of daily living (ADL); P 4, moderate to severe pain with frequent medication and occasional absence from work or significant change in ADL; and P 5, constant or severe incapacitating pain requiring chronic medication. The performance status was evaluated before and after the surgery using the Eastern Cooperative Oncology Group (ECOG) scale (PS 0–4) [18]: PS 0, normal activity; PS 1, symptomatic but almost completely ambulatory; PS 2, confined to bed less than 50% of normal daytime; PS 3, confined to bed more than 50% of normal daytime; and PS 4, confined to bed.

Lower limb motor strength was classified into the following groups: hip flexors, knee extensors, ankle extensors and flexors, and hallucis longus extensor and flexor. These groups were examined for weakness using the modified Medical Research Council's manual motor test (MMT) 0–5 grade [19]: MMT 0, no movement; MMT 1, a flicker of movement is seen or felt in the muscle; MMT 2, muscle moves the joint when gravity is eliminated; MMT 3, muscle cannot hold the joint against resistance, but moves the joint fully against gravity; MMT 4, muscle holds the joint against a combination of gravity and moderate resistance; and MMT 5, normal strength. Of the six muscle groups, the group showing the weakest muscular strength was selected and studied over time before and after the

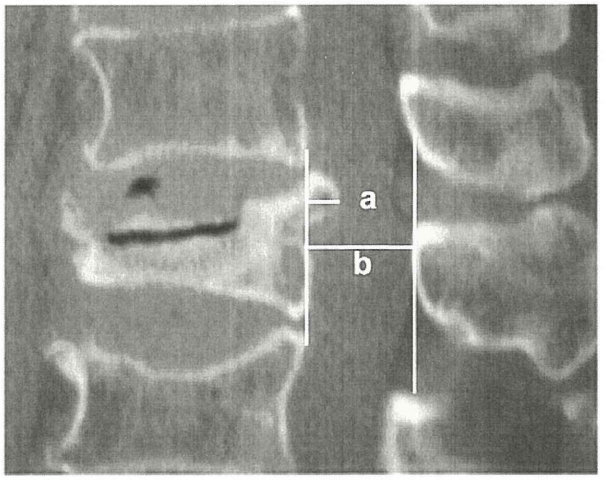

Fig. 3 Spinal canal encroachment rate estimated with sagittal CT reconstruction images. Spinal canal encroachment rate = retropulsed bone fragments (*a*)/spinal canal (*b*) × 100 (%)

surgery. Sensory and bladder dysfunctions were also evaluated before the surgery and at the latest follow-up visit.

Radiographic appearance

In preoperative evaluations, clefts were observed in the affected vertebrae of all patients in supine plain X-ray images and MR images were used to evaluate intravertebral components within the clefts and confirm pseudarthrosis (Fig. 2a, b). Instability was evaluated using differences in the local kyphotic angles between sitting, standing and supine positions. The local kyphotic angles were measured from the superior endplate of the vertebra one level above the injured vertebral body to the inferior endplate of the vertebral body one level below (Cobb's technique) [20]. Spinal canal encroachment was measured using sagittal CT scan images (Fig. 3).

Table 2 Evaluation of postoperative recoveries by Denis pain scale P (1–5)

Case number	Before surg.	After surg.	1 month	3 months	6 months	1 year	Latest
1	4	1	1	1	1	1	1
2	4	1	2	1	1	–	1
3	5	1	1	1	1	1	1
4	4	1	2	2	2	1	2
5	4	1	1	2	1	1	1
6	4	1	2	2	2	1	1
7	5	1	1	2	1	2	1
8	5	1	1	1	2	1	2
9	4	1	2	1	1	1	1
10	5	2	2	1	1	–	1
11	5	1	1	1	1	1	1

Case 2 moved away 9 months after the surgery. Case 10 died 6 months after the surgery

$P < 0.01$; before surg. versus 0, 1, 3, 6 months and 1 year following the surgery, or latest follow-up visit; Wilcoxon signed-rank test

Table 3 Evaluation of postoperative recoveries by performance status PS (0–4)

Case number	Before surg.	After surg.	1 month	3 months	6 months	1 year	Latest
1	3	1	1	1	1	1	1
2	2	1	1	1	1	–	1
3	4	1	1	1	1	1	1
4	3	1	2	2	2	2	2
5	2	1	1	1	1	1	1
6	2	1	1	1	1	1	1
7	4	2	2	2	2	1	1
8	4	2	2	2	1	2	2
9	2	1	1	1	1	1	1
10	4	3	3	3	3	–	3
11	4	1	1	1	1	1	1

Case 2 moved away 9 months after the surgery. Case 10 died 6 months after the surgery

$P < 0.01$; before surg. versus 0, 1, 3, 6 months and 1 year following the surgery, or latest follow-up visit; Wilcoxon signed-rank test

Clinical courses and imagings were studied before the surgery, immediately following the surgery, 1, 3, 6 months and 1 year following the surgery, and at the time of the latest follow-up visit. These images were observed three times each by three orthopaedists. The resulting mean intraobserver coefficient of variation (CV) and mean interobserver CVs were 6.45 and 4.55% for supine X-ray image analysis, 5.83 and 4.68% for sitting or standing position image analysis and 5.51 and 2.37% for encroachment analysis, respectively.

Statistical analysis

Results are expressed as mean ± standard deviation (SD). The effects of the surgery were assessed with the Wilcoxon signed-rank test. Statistical significances were set at $P < 0.05$. Calculations were performed with StatFlex ver. 6.0 software (Artech Co., Ltd, Osaka, Japan).

Results

The surgery lasted 25–90 min (average 46 min), with very little bleeding, and no severe systemic complications were observed during or after the surgery. In postoperative treatment, cases 1–9 began ambulation with simple casts on the day following the surgery, but cases 10 and 11 ambulated with body casts for 6 weeks to prevent adjacent vertebral fractures. The postoperative follow-up period ranged from 6 to 95 months (mean period 37.3 ± 27.2 months), follow-up is continuing at present, except for 3 patients: case 2, who moved away 9 months following the surgery; case 9, who died a natural death 1 year and 9 months following the surgery; and case 10, who died from heart failure 6 months following the surgery (Table 1).

Clinical findings

The pain ameliorated immediately following the surgery in all patients. Immediately following the surgery almost all patients showed an improved Denis pain scale score from P4 or P5 to P1, but occasional pain was experienced by one patient. One month following the surgery, some patients experienced temporary pain (Table 2). Significant improvements in performance status were also observed in almost all patients (cases 1–6, 9, 11: PS was 2–4 before the surgery and 1 after the surgery; cases 7, 8: PS was 4 before the surgery and 2 after the surgery; case 10: PS was 4 before the surgery and 3 after the surgery) (Table 3). Case 10 had hemiplegia. Some patients showed an increase in Denis pain scale concurrently with adjacent vertebral fractures, but the performance status did not exacerbate. In addition, the local

Table 4 Results of the preoperative and latest neurological examination

Case number	MMT										Sensory disturbance		BBD	
	Hip flexors		Knee extensors		Ankle extensors		Ankle flexors		HL extensor		HL flexor			
	Before (R/L)	Latest (R/L)	Before (R/L)	Latest (R/L)	Before (R/L)	Latest (R/L)	Before (R/L)	Latest (R/L)	Before (R/L)	Latest (R/L)	Before (R/L)	Latest (R/L)	Before	Latest	Before	Latest
1	5/5	5/5	5/5	5/5	5/5	5/5	5/5	5/5	3/1	5/5	4/1	5/5	+	−	−	−
2	4/3	5/5	5/3	5/5	1/2	4/4	2/2	5/5	1/1	4/4	1/2	5/4	+	+	−	−
3	5/5	5/5	5/5	5/5	3/3	5/5	2/2	5/5	1/1	5/5	1/1	5/5	+	−	+	−
4	4/4	5/5	3/4	5/5	5/5	3/3	5/5	5/5	3/3	5/5	5/5	5/5	+	+	−	−
5	5/5	5/5	5/5	5/5	3/3	5/5	5/5	5/5	2/2	5/5	5/5	5/5	+	+	−	−
6	5/5	5/5	5/5	5/5	3/1	5/5	5/5	4/3	4/1	5/5	5/5	5/5	+	+	−	−
7	5/5	5/5	4/4	5/5	0/0	0/0	0/0	3/3	0/0	0/1	0/0	3/3	+	+	−	−
8	4/3	5/5	4/3	5/5	4/3	5/5	4/4	5/5	4/4	5/5	4/3	5/5	+	+	−	−
9	5/5	5/5	5/5	5/5	5/5	5/5	5/5	5/5	2/5	5/5	3/5	5/5	+	+	−	−
10	3/2	4/2	3/2	4/2	3/2	4/2	3/2	4/2	3/2	4/2	5/2	5/2	+	+	−	−
11	2/2	4/3	2/2	4/3	3/3	4/4	4/4	4/4	1/1	4/4	2/2	4/4	+	+	−	−

MMT manual muscle testing, *HL extensor* hallucis longus extensor, *HL flexor* hallucis longus flexor, *BBD* bladder and bowel dysfunction, *R/L* right/left, + present, − absent

kyphotic angles exacerbated, but significant improvements in motor weakness were observed in all patients at the latest follow-up visit. Although motor paralysis did not recover immediately following the surgery, the grades of muscle strength in the weakest muscles gradually improved over the examination period (cases 1, 3–6, 8, 9, 11: MMT was 1–3 before and immediately following the surgery and 5 at 1 year following the surgery; and case 7: MMT was 0 before and following the surgery and 0–3 at 1 year following the surgery) (Tables 4, 5). On performing a neurologic examination, no sensory disturbances were observed in any of the cases except two (cases 1 and 3) and one (case 3) with bladder dysfunction that completely recovered immediately following the surgery. Although the latter patient had difficulty in urination before surgery, it may have been caused by cystoplegia. Severe pain ($P = 5$) may cause difficulty in urination when a patient is confined to bed (Table 4).

Radiological findings

Ten vertebrae had low T1 and high T2 areas in the intravertebral cleft that were regarded as fluid accumulation (cases 1, 2, 4–11) and 1 vertebra showed low T1 and low T2 areas that were regarded as gas pattern (case 3) (Fig. 2). In preoperative CT scan images, spinal canal encroachment was 23.3–53.0% with a mean of 41.4 ± 11.0% (Table 6). A sagittal MR image

Table 5 Time course of muscle strength recoveries MMT (0–5) of the weakest muscle groups before surgery

Case number	Weakest muscle groups	Before surg.	After surg.	1 month	3 months	6 months	1 year	Latest
1	H/E, H/F	1	1	2	3	5	5	5
2	A/E, H/E	1	1	3–4	3	4	–	4
3	H/E, H/F	1	1	2	2	5	5	5
4	H/E, H/F	1	1	4	4	5	5	5
5	H/E	2	2	2	4	4	5	5
6	A/E, H/E	1	1	1	3	5	5	5
7	A/E, A/F, H/E, H/F	0	0	0–2	0–2	0–3	0–3	0–3
8	K/E, H/E	3	3	3	3–4	5	5	5
9	H/E	2	2	5	5	5	5	5
10	Hi/F, K/E, A/E, A/F, H/E, H/F	3	3	4	4	4	–	4
11	H/E	1	1	3	4	5	5	5

Case 2 moved away 9 months after the surgery. Case 10 died 6 months after the surgery

Hi/F hip flexors, *K/E* knee extensors, *A/E* ankle extensors, *A/F* ankle flexsors, *H/E* hallucis longus extensor, *H/F* hallucis longus flexor, *MMT scale* manual muscle testing

Table 6 Pre- and postoperative X-ray examination

Case number	Encroachment (%)	Kyphotic angle (supine) (°)		Kyphotic angle (sitting or standing) (°)			Instability angle (°)		Bridging callus (months)
		Before	After	Before	After	6 months after	Before	After	
1	46.5	22.0	24.3	35.5	29.0	28.8	13.5	5.3	3
2	38.0	6.0	9.3	16.5	12.0	17.3	10.5	3.8	6
3	50.5	3.3	5.5	16.8	8.8	16.0	13.5	3.8	3
4	48.5	3.0	5.8	15.0	8.8	14.8	12.0	3.5	1
5	47.3	31.0	38.5	50.8	41.3	57.5	19.8	4.3	3
6	47.5	27.3	31.0	50.3	34.3	35.0	23.0	4.3	3
7	23.3	20.0	27.3	59.8	30.5	39.8	39.8	4.5	6
8	25.0	23.0	29.8	45.3	33.0	45.0	22.3	3.8	6
9	48.0	12.5	15.8	45.0	20.5	46.8	32.5	4.8	6
10	53.0	20.0	20.5	31.5	24.5	24.3	11.5	4.3	3
11	27.5	6.3	8.8	19.3	13.3	12.3	13.0	4.8	3
Mean ± SD	41.4 ± 11.0	15.8 ± 10.0	19.7 ± 11.4	35.0 ± 16.2	23.3 ± 11.3	30.7 ± 15.2	19.2 ± 9.6	4.3 ± 0.5	3.0 ± 3.0

Instability angle the difference between the local kyphotic angle of sitting (or standing) position and supine

showed no decrease of encroachment after the surgery (Fig. 6a, b). Instabilities were visible in the preoperative X-rays in all cases, 10.5–39.8° with a mean of 19.2 ± 9.6°, and were significantly reduced following the surgery, 3.5–5.3° with a mean of 4.3 ± 0.5° (Table 6). Instability angles significantly improved ($P < 0.01$) (Fig. 4). Kyphotic angles in the sitting or standing positions before the surgery, 15.0–59.8° with a mean of 35.0 ± 16.2°, significantly improved the surgery, 8.8–41.3° with a mean of 23.3 ± 11.3° (Table 6; Figs. 4, 5a, b). At 6 months following the surgery, kyphotic angles were 12.3–57.5° with a mean of 30.7 ± 15.2° (Table 6; Fig. 5c). Seven of the 11 cases showed an increase in kyphotic angles because of adjacent vertebral fractures, whereas 2 of 11 cases, put in body casts, did not have further vertebral fractures following the surgery. Bridging callus formation was observed in all cases until 6 months following the surgery, i.e. 1–6 months with a mean of 3.0 ± 3.0 months (Table 6; Fig. 5d).

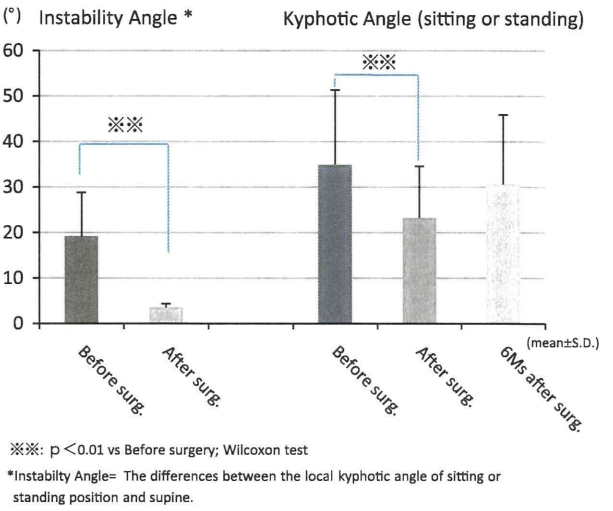

Fig. 4 Instability angles were significantly improved by the surgery. Kyphotic angles were initially realigned (significant difference), but correction loss occurred at 6 months after the surgery because of adjacent vertebral fractures

Discussion

In this study, significant pain was immediately ameliorated whereas motor analysis was ameliorated within 6 months following percutaneous vertebroplasty in 11 subjects with delayed-onset motor paralysis. Regarding neurologic symptoms, two cases showed complete improvement including sensory disturbance and muscular strength in all cases except one within the examination period. The surgery was, therefore, considered to be very effective. All the unstable vertebrae were apparently stabilized by the surgery. However, comparing pre- and postoperative MR images of the subjects showed no visible change in the pressure of the spinal canal. The kyphotic angles transiently improved immediately following the surgery, but correction loss occurred in 7 of 11 cases. Thus, stabilizing the vertebra is the most important factor to remedy a neural deficit.

Osteoporotic vertebral pseudarthrosis is recognized as bone necrosis following a vertebral compression fracture and the unstable kyphotic vertebra sometimes causes persistent pain or neural disturbances [1, 4]. Delayed-onset paraplegia following vertebral collapse is caused by neural compression due to retropulsed bone fragments in the spinal canal, progression of kyphosis and instability at the fracture site [6–8]. Ataka et al. [21] reported an amelioration of the neurologic symptoms of 14 cases having osteoporotic vertebral fracture with motor paralysis using treatment only with posterior fusion without decompression, whereas decompression of the spinal cord by laminectomy failed to relieve the neural symptoms [5, 10]. In this study, we clarified that stabilizing the concerned vertebra ameliorated the neural disturbances in all cases, the largest encroachment of which was 53% of case 10. Thus, stabilizing the unstable vertebra is more effective in relieving paralysis than decompression of the spinal cord if the encroachment of the spinal canal was less than 50%. However, one case which had remarkably poor neurological conditions during the preoperative period insufficiently improved motor paralysis in spite of the operation (case 7). The fracture site in this case was the most unstable and complete motor paralysis was widespread. Thus, wide and complete motor deficits might mean irreversible paralysis from which it is difficult to expect complete recovery as a result of the vertebroplasty. Moreover, if a large instability angle was shown at the fracture site, earlier stabilization might be needed to prevent irreversible nerve injuries.

Correction loss was observed in 7 of 11 cases because of fractures of the adjacent vertebrae, and the kyphotic angles on the latest follow-up visit were greater than those before the surgery in 6 of 7 cases. The increase in kyphotic angles did not affect muscle strength recovery, pain score or performance status. Although ADL were not affected by kyphotic changes in this study, Miyakoshi et al. [22] reported the importance of spinal alignment to maintain ADL. Thus, increase in kyphotic changes may cause inconvenience in certain situations and lifestyles. Tanigawa et al. [23] reported that a new vertebral body fracture following percutaneous vertebroplasty for a vertebral fracture with cleft was observed in 50% of the cases. In osteoporotic patients, previous fracture elevated the risk of sequential fractures in other parts [24], which is prevented by antiresorptive agents, particularly bisphosphonates [25, 26]. Also, intermittent administration of parathyroid hormone may suppress an increase in kyphotic angles following vertebroplasty [27]. In 2 cases using body casts, we prevented correction loss. Thus,

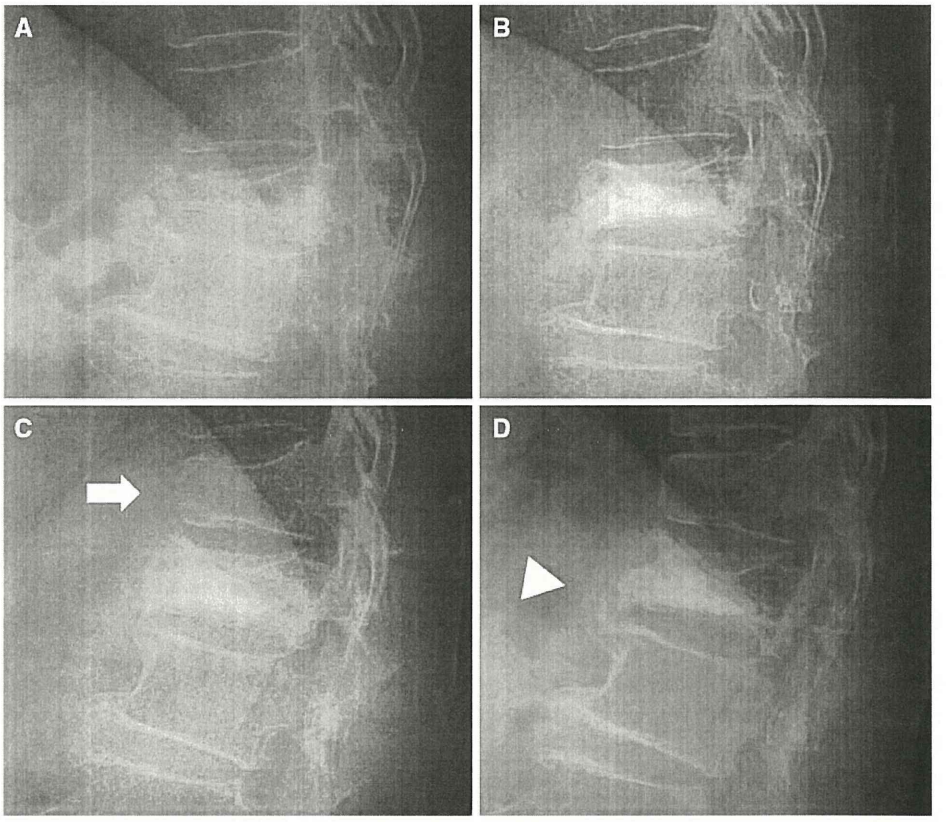

Fig. 5 Lateral X-ray image in sitting position shows collapsed vertebra of the L1 body (**a**), kyphotic angles are realigned by vertebroplasty (**b**), adjacent vertebral fracture 3 months after the surgery (**c**), bridging callus formation on the front of vertebrae at 1 year after the surgery (**d**). Adjacent vertebral fracture occurred (*arrow*). Bridging callus appeared (*arrowhead*)

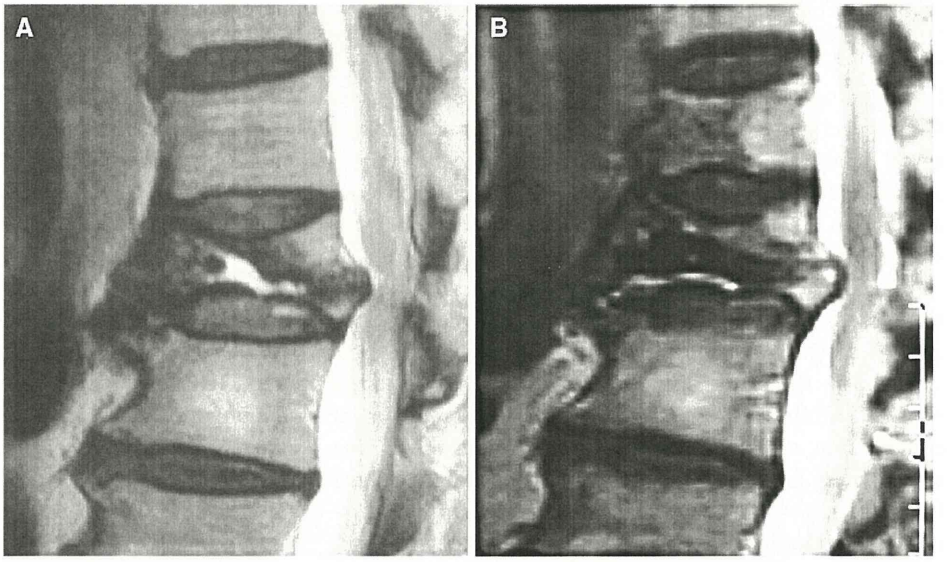

Fig. 6 Sagittal T2-weighted MR image demonstrates spinal cord encroachment by bone fragments before (**a**) and after the surgery (**b**)

realignment of the spine following osteoporotic vertebral fractures by vertebroplasty may be kept without long spinal fusion if antiosteoporotic agents or body casts are prescribed.

This study has some limitations. Pseudarthrosis occurs in about 10% of all vertebral fractures [1] and the probability of it being complicated with delayed-onset paraplegia is lower; therefore, we could not verify the effectiveness of this surgery as a case control, randomized control or sequential study. However, the most important point of this study is that all 11 patients with delayed-onset paraplegia following osteoporotic vertebral fracture were relieved of inconvenience of daily living with a less invasive surgery. Although the usefulness of the percutaneous vertebroplasty for the treatment of painful osteoporotic vertebral compression

fractures remains controversial [28–30], we believe that following vertebral fracture with delayed-onset paraplegia it is a useful procedure despite the small sample size used in this study.

Acknowledgments The authors did not receive any benefits or funding from any commercial party related directly or indirectly to the subject of this article.

References

1. Libicher M, Appelt A, Berger I, Baier M, Meeder PJ, Grafe I, Dafonseca K, Noldge G, Kasperk C. The intravertebral vacuum phenomen as specific sign of osteonecrosis in vertebral compression fractures: results from a radiological and histological study. Eur Radiol. 2007;17:2248–52.
2. Maldague BE, Noel HM, Malghem JJ. The intravertebral vacuum cleft: a sign of ischemic vertebral collapse. Radiology. 1978;129:23–9.
3. Hasegawa K, Homma T, Uchiyama S, Takahashi H. Vertebral pseudarthrosis in the osteoporotic spine. Spine (Phila Pa 1976). 1998;23:2201–6.
4. Steel HH. Kummell's disease. Am J Surg. 1951;81:161–7.
5. Kempinsky WH, Morgan PP, Boniface WR. Osteoporotic kyphosis with paraplegia. Neurology. 1958;8:181–6.
6. Sutherland CJ, Miller F, Wang GJ. Early progressive kyphosis following compression fractures. Two case reports from a series of "stable" thoracolumbar compression fractures. Clin Orthop Relat Res. 1983;173:216–20.
7. Tanaka S, Kubota M, Fujimoto Y, Hayashi J, Nishikawa K. Conus medullaris syndrome secondary to an L1 burst fracture in osteoporosis. A case report. Spine (Phila Pa 1976). 1993;18:2131–4.
8. Mochida J, Toh E, Chiba M, Nishimura K. Treatment of osteoporotic late collapse of a vertebral body of thoracic and lumbar spine. J Spinal Disord. 2001;14:393–8.
9. Kaneda K, Asano S, Hashimoto T, Satoh S, Fujiya M. The treatment of osteoporotic-posttraumatic vertebral collapse using the Kaneda device and a bioactive ceramic vertebral prosthesis. Spine (Phila Pa 1976). 1992;17:S295–303.
10. Shikata J, Yamamuro T, Iida H, Shimizu K, Yoshikawa J. Surgical treatment for paraplegia resulting from vertebral fractures in senile osteoporosis. Spine (Phila Pa 1976). 1990;15:485–9.
11. Jensen ME, Evans AJ, Mathis JM, Kallmes DF, Cloft HJ, Dion JE. Percutaneous polymethylmethacrylate vertebroplasty in the treatment of osteoporotic vertebral body compression fractures: technical aspects. AJNR Am J Neuroradiol. 1997;18:1897–904.
12. Barr JD, Barr MS, Lemley TJ, McCann RM. Percutaneous vertebroplasty for pain relief and spinal stabilization. Spine (Phila Pa 1976). 2000;25:923–8.
13. Garfin SR, Yuan HA, Reiley MA. New technologies in spine: kyphoplasty and vertebroplasty for the treatment of painful osteoporotic compression fractures. Spine (Phila Pa 1976). 2001;26:1511–5.
14. Jang JS, Kim DY, Lee SH. Efficacy of percutaneous vertebroplasty in the treatment of intravertebral pseudarthrosis associated with noninfected avascular necrosis of the vertebral body. Spine (Phila Pa 1976). 2003;28:1588–92.
15. Lane JI, Maus TP, Wald JT, Thielen KR, Bobra S, Luetmer PH. Intravertebral clefts opacified during vertebroplasty: pathogenesis, technical implications, and prognostic significance. AJNR Am J Neuroradiol. 2002;23:1642–6.
16. FDA Public Health Web Norification. Complications related to the use of bone cement and bone void fillers in treating compression fractures of the spine. 2004. http://www.fda.gov/cdrh/safety/bonecement.html; http://www.fda.gov/cdrh/.
17. Denis F, Armstrong GW, Searls K, Matta L. Acute thoracolumbar burst fractures in the absence of neurologic deficit. A comparison between operative and nonoperative treatment. Clin Orthop Relat Res. 1984;(189):142–9.
18. Verger E, Salamero M, Conill C. Can Karnofsky performance status be transformed to the Eastern Cooperative Oncology Group scoring scale and vice versa? Eur J Cancer. 1992;28A:1328–30.
19. Florence JM, Pandya S, King WM, Robison JD, Baty J, Miller JP, Schierbecker J, Signore LC. Intrarater reliability of manual muscle test (Medical Research Council scale) grades in Duchenne's muscular dystrophy. Phys Ther. 1992;72:115–22.
20. Kuklo TR, Polly DW, Owens BD, Zeidman SM, Chang AS, Klemme WR. Measurement of thoracic and lumbar fracture kyphosis: evaluation of intraobserver, interobserver, and technique variability. Spine (Phila Pa 1976). 2001;26:61–5.
21. Ataka H, Tanno T, Yamazaki M. Posterior instrumented fusion without neural decompression for incomplete neurological deficits following vertebral collapse in the osteoporotic thoracolumbar spine. Eur Spine J. 2009;18:69–76.
22. Miyakoshi N, Hongo M, Maekawa S, Ishikawa Y, Shimada Y, Itoi E. Back extensor strength and lumbar spinal mobility are predictors of quality of life in patients with postmenopausal osteoporosis. Osteoporos Int. 2007;18:1397–403.
23. Tanigawa N, Komemushi A, Kariya S, Kojima H, Shomura Y, Omura N, Sawada S. Relationship between cement distribution pattern and new compression fracture after percutaneous vertebroplasty. AJR Am J Roentgenol. 2007;189:W348–52.
24. Klotzbuecher CM, Ross PD, Landsman PB, Abbott TA 3rd, Berger M. Patients with prior fractures have an increased risk of future fractures: a summary of the literature and statistical synthesis. J Bone Miner Res. 2000;15:721–39.
25. Watts NB, Josse RG, Hamdy RC, Hughes RA, Manhart MD, Barton I, Calligeros D, Felsenberg D. Risedronate prevents new vertebral fractures in postmenopausal women at high risk. J Clin Endocrinol Metab. 2003;88:542–9.
26. Black DM, Cummings SR, Karpf DB, Cauley JA, Thompson DE, Nevitt MC, Bauer DC, Genant HK, Haskell WL, Marcus R, Ott SM, Torner JC, Quandt SA, Reiss TF, Ensrud KE. Randomised trial of effect of alendronate on risk of fracture in women with existing vertebral fractures. Fracture Intervention Trial Research Group. Lancet. 1996;348:1535–41.
27. Neer RM, Arnaud CD, Zanchetta JR, Prince R, Gaich GA, Reginster JY, Hodsman AB, Eriksen EF, Ish-Shalom S, Genant HK, Wang O, Mitlak BH. Effect of parathyroid hormone (1–34) on fractures and bone mineral density in postmenopausal women with osteoporosis. N Engl J Med. 2001;344:1434–41.
28. Buchbinder R, Osborne RH, Ebeling PR, Wark JD, Mitchell P, Wriedt C, Graves S, Staples MP, Murphy B. A randomized trial of vertebroplasty for painful osteoporotic vertebral fractures. N Engl J Med. 2009;361:557–68.
29. Kallmes DF, Comstock BA, Heagerty PJ, Turner JA, Wilson DJ, Diamond TH, Edwards R, Gray LA, Stout L, Owen S, Hollingworth W, Ghdoke B, Annesley-Williams DJ, Ralston SH, Jarvik JG. A randomized trial of vertebroplasty for osteoporotic spinal fractures. N Engl J Med. 2009;361:569–79.
30. Klazen CA, Lohle PN, de Vries J, Jansen FH, Tielbeek AV, Blonk MC, Venmans A, van Rooij WJ, Schoemaker MC, Juttmann JR, Lo TH, Verhaar HJ, van der Graaf Y, van Everdingen KJ, Muller AF, Elgersma OE, Halkema DR, Fransen H, Janssens X, Buskens E, Mail WP. Vertebroplasty versus conservative treatment in acute osteoporotic vertebral compression fractures (Vertos): an open-label randomised trial. Lancet. 2010;376:1085–92.

Dopamine Induces IL-6–Dependent IL-17 Production via D1-Like Receptor on CD4 Naive T Cells and D1-Like Receptor Antagonist SCH-23390 Inhibits Cartilage Destruction in a Human Rheumatoid Arthritis/SCID Mouse Chimera Model

Kazuhisa Nakano,* Kunihiro Yamaoka,* Kentaro Hanami,* Kazuyoshi Saito,* Yasuyuki Sasaguri,† Nobuyuki Yanagihara,‡ Shinya Tanaka,§ Ichiro Katsuki,¶ Sho Matsushita,‖ and Yoshiya Tanaka*

A major neurotransmitter dopamine transmits signals via five different seven-transmembrane G protein-coupled receptors termed D1–D5. Several studies have shown that dopamine not only mediates interactions into the nervous system, but can contribute to the modulation of immunity via receptors expressed on immune cells. We have previously shown an autocrine/paracrine release of dopamine by dendritic cells (DCs) during Ag presentation to naive $CD4^+$ T cells and found efficacious results of a D1-like receptor antagonist SCH-23390 in the experimental autoimmune encephalomyelitis mouse model of multiple sclerosis and in the NOD mouse model of type I diabetes, with inhibition of Th17 response. This study aimed to assess the role of dopaminergic signaling in Th17-mediated immune responses and in the pathogenesis of rheumatoid arthritis (RA). In human naive $CD4^+$ T cells, dopamine increased IL-6–dependent IL-17 production via D1-like receptors, in response to anti-CD3 plus anti-CD28 mAb. Furthermore, dopamine was localized with DCs in the synovial tissue of RA patients and significantly increased in RA synovial fluid. In the RA synovial/SCID mouse chimera model, although a selective D2-like receptor antagonist haloperidol significantly induced accumulation of IL-6^+ and IL-17^+ T cells with exacerbated cartilage destruction, SCH-23390 strongly suppressed these responses. Taken together, these findings indicate that dopamine released by DCs induces IL-6–Th17 axis and causes aggravation of synovial inflammation of RA, which is the first time, to our knowledge, that actual evidence has shown the pathological relevance of dopaminergic signaling with RA. ***The Journal of Immunology*****, 2011, 186: 3745–3752.**

Dopamine is the major neurotransmitter in the CNS, and it is involved in the control of locomotion, emotion, cognition, and neuroendocrine secretion (1, 2). The CNS and the neurotransmitters have been previously reported to control the immune system and to regulate host defense (3–5). Receptors for various neurotransmitters are expressed on the cell surface of lymphocytes, indicating the importance of such neuroimmune interactions (6–12). Dopamine receptors are seven-transmembrane G protein-coupled receptors and five subtypes from D1 to D5 (2, 13). These subtypes are classified into two subgroups. D1 and D5 are D1-like receptors that coupled to Gαs, which increases intracellular cAMP. In contrast, D2, D3, and D4 are D2-like receptors that coupled to Gαi, which decreases intracellular cAMP (2, 13). Dopaminergic signaling via D2-like receptors coupled to the inhibition cAMP production in T lymphocytes often has an immunostimulatory effect (7, 8, 10). Conversely, signaling via D1-like receptors coupled to increasing cAMP promotes the inhibition of the immune response (8). Dopamine has been shown to inhibit proliferation of human lymphocytes, and even to induce apoptosis in peripheral mononuclear cells (14, 15). Studies carried out on human and murine lymphocytes have demonstrated that these cells express all subtypes of dopamine receptors (10, 14, 16–19). However, most of these results are still inconclusive and even contradictory. Lymphocytes are a mixture of different classes and functional subsets. Different lymphocyte classes and subsets may express different dopamine receptor subtypes. Furthermore, differences in ligand binding affinity, basal activity, efficacy, G protein activation, desensitization, and internalization rates may be expected to be discriminating properties of the dopamine receptors. Because these variations and differences of dopamine receptors sometimes make interpretation of data extremely difficult, immunomodulation by dopamine needs to be investigated with each lymphocyte subset.

*The First Department of Internal Medicine, School of Medicine, University of Occupational and Environmental Health, Kitakyushu 807-8555, Japan; †Department of Pathology and Cell Biology, School of Medicine, University of Occupational and Environmental Health, Kitakyushu 807-8555, Japan; ‡Department of Pharmacology, School of Medicine, University of Occupational and Environmental Health, Kitakyushu 807-8555, Japan; §Department of Orthopedic Surgery, School of Medicine, University of Occupational and Environmental Health, Kitakyushu 807-8555, Japan; ¶Department of Orthopedic Surgery, Nippon Steel Yawata Memorial Hospital, Kitakyushu 805-8508, Japan; and ‖Department of Allergy and Immunology, Faculty of Medicine, Saitama Medical University, Saitama 350-0495, Japan

Received for publication July 23, 2010. Accepted for publication January 8, 2011.

This work was supported by a Research Grant-In-Aid for Scientific Research by the Ministry of Health, Labor and Welfare of Japan, the Ministry of Education, Culture, Sports, Science and Technology of Japan, and the University of Occupational and Environmental Health, Japan.

Address correspondence and reprint requests to Prof. Yoshiya Tanaka, University of Occupational and Environmental Health, School of Medicine, 1-1 Iseigaoka, Yahatanishi-ku, Kitakyushu 807-8555, Japan. E-mail address: tanaka@med.uoeh-u.ac.jp

Abbreviations used in this article: DC, dendritic cell; EAE, experimental autoimmune encephalomyelitis; OA, osteoarthritis; RA, rheumatoid arthritis; SCID-HuRAg, SCID mice engrafted with human RA synovium; Treg, regulatory T cell; WST-8, 2-(2-methoxy-4-nitrophenyl)-3-(4-nitrophenyl)-5-(2,4-disulfophenyl)-2H-tetrazolium.

www.jimmunol.org/cgi/doi/10.4049/jimmunol.1002475

$CD4^+$ T cells, on activation and expansion, develop into different Th cell subsets with different cytokine profiles and distinct effector functions. Th17 cells are the newest member of the effector Th cell family and are characterized by their ability to produce specific cytokines such as IL-17, IL-22, IL-17F, IL-21, and CCL20. TGF-β, IL-6, IL-1β, IL-21, and IL-23 are important for the polarization of Th17 cells from human $CD4^+$ naive T cells (20, 21), and the absence of TGF-β mediates a shift from a Th17 profile to a Th1 profile (21, 22). Recent studies have demonstrated that Th17 cells, rather than Th1 cells, play a pivotal role in the pathogenesis of autoimmune disease models, including experimental autoimmune encephalomyelitis (EAE) and collagen-induced arthritis (23, 24). Furthermore, a number of observations suggest that Th17 cytokines may be important in rheumatoid arthritis (RA), a representative human autoimmune inflammatory disease. IL-17 is found in RA synovial fluid and in the T cell-rich areas of RA synovial tissue (25–28). In RA patients, in a 2-y prospective study, the cytokine expression of TNF-α, IL-1β, and IL-17 was predictive of joint destruction, whereas IFN-γ was protective (29). Although the direct proinflammatory effects of IL-17 are often small when compared with those of IL-1β and TNF-α, IL-17 may enhance the effects of other cytokines. Using RA synovial tissue fibroblasts, IL-17 enhanced IL-1–mediated IL-6 and CCL20 production (30, 31) and the TNF-α–induced synthesis of IL-1β, IL-6, IL-8, and CCL20 (31, 32), indicating that the effects of IL-17 may be caused by its ability to promote inflammation by inducing cytokines and chemokines (33, 34). Furthermore, direct effector functions of Th17 cells in RA have been demonstrated in that receptor activator for NF-κB ligand (RANKL) expression on the surface of Th17 cells induces osteoclastogenesis (25, 35, 36), promoting cartilage and bone destruction independently of TNF-α and IL-1β (37, 38). These proinflammatory cytokines induced by IL-17 might even feedback on the generation and expansion of further Th17 cells in this specific microenvironment of the joint. Actually, initial observations from phase I trials show that signs and symptoms of RA are significantly suppressed after treatment with anti–IL-17 Abs, without notable adverse effects, indicating that IL-17 is an important therapeutic target for the treatment of RA (39).

Dendritic cells (DCs) are the most powerful APCs that determine the balance of differentiation of Th cell subsets. In particular, cytokines produced by DCs are regarded as the key to T cell differentiation. For example, IL-12 produced by DCs induces the differentiation to Th1 (40). In our previous studies, we showed that human monocyte-derived DCs stored dopamine, and that dopamine was released on Ag-specific interaction with naive $CD4^+$ T cells (41). Furthermore, antagonizing dopamine receptor subtypes differentially affected Th17 polarization in vitro (19). D2-like receptor antagonists judged to be Th17 adjuvants in vitro caused a marked deterioration of EAE, whereas D1-like receptor antagonists exhibited a marked improvement in EAE (19). Although the precise mechanism of how D1-like receptor antagonists inhibit IL-17 production remains undetermined, our previous results indicated that DC-derived dopamine might induce the differentiation to Th17.

In this study, we show that dopamine induces IL-6–dependent IL-17 production in vitro, and that antagonizing D1-like receptor inhibits dopamine-mediated IL-6–Th17 axis in vitro and in a human RA/SCID mouse chimera model.

Materials and Methods

Purification of human naive $CD4^+$ T lymphocytes

The study using peripheral blood of healthy volunteers was approved by the Human Subjects Research Committee of the University of Occupational and Environmental Health, Japan. Highly purified, untouched $CD4^+$ T cells were prepared from PBMCs of healthy volunteers by exhaustive immunomagnetic negative selection. We routinely used AutoMACS separation columns (Miltenyi Biotec, Germany) and a $CD4^+$ T cell Isolation Kit II (Miltenyi Biotec), and separated into $CD45RO^+$ memory T cells and $CD45RA^+$ naive T cells using $CD45RO^+$ MicroBeads (Miltenyi Biotec). A FACSCalibur flow cytometer (BD Biosciences) showed the purity of these cells to be >99%.

Synovial tissues and treatments

Synovial tissues were obtained from patients with active RA, diagnosed according to the criteria of the American College of Rheumatology (formerly the American Rheumatism Association) (42), undergoing joint replacement or synovectomy. This study was approved by the Human Subjects Research Committee of our university. Informed consent was obtained from all subjects enrolled in the study. Synovial membrane samples were perfused with 5% glutaraldehyde, and paraffin sections (3 μm thick) were prepared for immunohistochemical studies. Synovial membrane and cartilage were also dissected under sterile conditions in PBS and immediately prepared for coimplantation to SCID mice.

Cell cultures

Synovial tissues samples were dissected under sterile conditions in PBS and immediately prepared for culture of fibroblast-like synovial cells. In brief, the tissue sample was minced into small pieces and digested with collagenase (Sigma Aldrich Japan, Tokyo) in serum-free DMEM (Life Technologies BRL, Grand Island, NY). After filtering through a nylon mesh, the cells were extensively washed and suspended in DMEM, supplemented with 10% FCS (Bio-Pro, Karlsruhe, Germany). Finally, isolated cells were seeded in 25-cm^2 culture flasks (Falcon, Lincoln Park, NJ) and cultured in a humidified 5% carbon dioxide atmosphere. After overnight culture, nonadherent cells were removed and incubation of adherent cells was continued in a fresh medium. At confluence, the cells were trypsinized, passaged at a 1:3 split ratio, and recultured. The medium was changed twice each week, and the cells were used after three to five passages.

Quantitative analysis of IFN-γ, IL-5, IL-17, IL-1β, TGF-β1, and IL-6

Cytokine concentrations in culture supernatant were measured by ELISA kit (R&D Systems).

Quantitative real-time PCR

Total RNA was extracted using the RNeasy mini kit (Qiagen, Tokyo, Japan), according to the manufacturer's instructions. cDNA was reverse transcribed using the high-capacity RNA-to-cDNA Master Mix (Applied Biosystems, Tokyo, Japan). Primers and probes were all predesigned TaqMan Gene Expression Assays from Applied Biosystems. Real-time PCR was performed on the StepOnePlus Real-Time PCR System (Applied Biosystems) machine. Predeveloped specific primers were used to detect *rorc* (Hs01076112) and 18s (Hs99999901). Target gene expression was normalized using 18s expression level and expressed in arbitrary units.

Cell viability assay

Cell viability was assessed using a TetraColor One kit including WST-8 [2-(2-methoxy-4-nitrophenyl)-3-(4-nitrophenyl)-5-(2,4-disulfophenyl)-2H-tetrazolium] and electron carrier mixture (Seikagaku, Tokyo, Japan). The WST-8 assay is based on the conversion of tetrazolium salt WST-8 to the highly water-soluble formazan. Cells (1×10^5) were seeded and incubated on a 96-well flat-bottom plate (Iwaki) in DMEM containing 10% FCS in a final volume of 0.1 ml for 24 h at 37°C. They were treated with different agents for various time intervals. Ten milliliters of a solution containing 5 mM WST-8, 0.2 mM 1-methoxy-5-methylphenazium methosulfate, and 150 mM NaCl was added to each well. After incubation for 2 h at 37°C, the OD of each well was measured on a microplate reader at 450 nm.

Flow cytometric detection of cell-surface dopamine receptors

Staining and flow cytometric analysis of synovial fibroblasts were carried out by standard procedures as already described using a FACSCalibur (BD Biosciences). Anti-dopamine D1–D5 receptor rabbit polyclonal Abs were obtained from Calbiochem. In brief, synovial fibroblasts (1×10^5 cells/sample) were incubated with anti-dopamine receptor polyclonal Ab for 20 min at 4°C, followed by FITC-conjugated anti-rabbit IgG (Sigma) at saturating concentrations in FACS medium consisting of HBSS (Nissui, Tokyo, Japan), 0.5% human serum albumin (Mitsubishi Pharma, Osaka,

Japan), and 0.2% NaN_3 (Sigma) for 20 min at 4°C. After three washes in FACS medium, the cells were analyzed with the FACSCalibur.

Fractional catecholamine analysis

Ten patients with RA and 10 control patients with osteoarthritis (OA) were diagnosed according to the American College of Rheumatology criteria (42). Synovial fluid specimens were collected during either diagnostic or therapeutic arthrocentesis of the knee (10 knees in 10 cases with RA and 10 knees in 10 cases with OA; Table I). All synovial samples were collected under sterile conditions, and the cellular components were removed immediately after centrifugation. The supernatants were stored at −30°C. The supernatants were transferred immediately to a test tube containing perchloric acid (final concentration, 0.4 M). Catecholamines (dopamine, noradrenaline, and adrenaline) were adsorbed onto aluminum hydroxide and estimated by the ethylenediamine condensation method using a fluorescence spectrophotometer (F-4010; Hitachi, Tokyo, Japan) with excitation and emission wavelengths of 420 and 540 nm, respectively (43).

Preparation of human RA/SCID chimera mice and treatment with dopamine receptor antagonists

Human RA/SCID chimera mice were evaluated as models for the treatment study. A total of 18 male SCID mice (CR.17/lcr; CLEA Japan, Tokyo, Japan), 6- to 7-wk-old, which had been bred under specific pathogen-free conditions at our university animal center, were used for establishment of the human RA/SCID chimera mouse model. Pannus tissue from synovial membrane, cartilage, and bone, collected as a mass from RA patients at the time of surgery, was used for implantation. The size of the removed specimen was adjusted to a block almost 4–8 mm in diameter before implantation. The mice were anesthetized with diethyl ether, according to the guidelines established by the animal ethics committee of the University of Occupational and Environmental Health, Japan. The tissue implants were grafted s.c. on the backs of the mice. All surgical procedures were performed under sterile conditions. The mice were randomly assigned to three groups at 1 wk after the implantation. The mice in the test groups were s.c. administered 0.3 mg/kg haloperidol (a D2-like receptor antagonist; Sigma, Japan) or 0.3 mg/kg SCH-23390 (a D1-like receptor antagonist; Sigma) twice a week for 3 wk. The mice in the control group received 50 μl PBS. Thirty days after implantation, the mice were anesthetized and their implanted tissues were removed. The animal experiments were approved by and performed in compliance with the guidelines of the Institutional Animal Care and Use Committee.

Histochemical analysis

The 3-μm-thick sections prepared from RA synovial tissues were incubated with rabbit anti-dopamine Ab (Chemicon) or S-100 and then incubated with secondary Ab (EnVision+; Dako) (44, 45). The implanted tissues were removed and histologically observed after H&E staining. To examine biological activities of the implanted tissues, we performed immunohistochemical staining as previously described (44, 45). The sections were stained with the following anti-human monoclonal Abs and an immunostaining kit: IFN-γ, IL-17, IL-6, and EnVision+. These were purchased from Dako Japan.

Statistical analysis

Parametric testing among three or more groups was performed by ANOVA. Nonparametric testing was performed using the Mann–Whitney rank sum test.

Results

Dopamine increases IL-6–dependent IL-17 secretion from human T cells

We have previously reported that only D1 was specifically expressed at a high level in $CD4^+$ naive T cells, and that dopamine increased the cAMP concentrations in $CD4^+$ naive T cells via D1-like receptors, and subsequently induced the secretion of IL-4 and IL-5 (19, 41). In this study, we first examined the pattern of cytokine secretion including IL-17 from $CD4^+$ naive T cells, which were stimulated by anti-CD3/CD28 Abs and simultaneously added dopamine. Dopamine slightly increased IL-5 secretion without affecting IFN-γ production, whereas dopamine markedly increased IL-17 secretion in a dose-dependent manner, indicating dopamine as an important factor for Th17 differentiation rather than Th2 differentiation (Fig. 1*A*). We also measured the concentration of Th17-inducible cytokines such as IL-6, IL-1β, and TGF-β. Interestingly, IL-6 secretion also increased in a dose-dependent manner (Fig. 1*B*), whereas minimum IL-1β and no TGF-β secretion were observed (data not shown). At the same time, we investigated the response of naive human T cells to

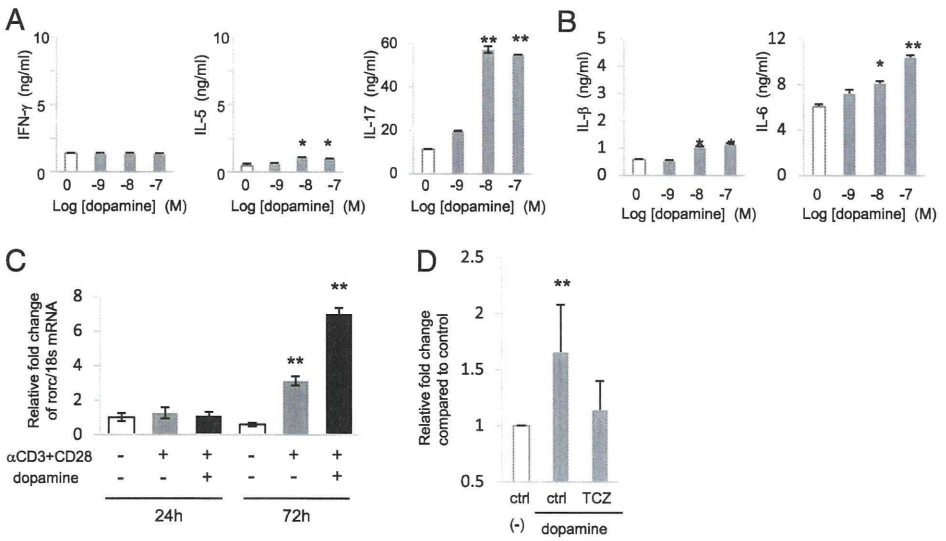

FIGURE 1. Dopamine-mediated cytokine secretion from $CD4^+$ T cells. Purified human $CD4^+$ naive T cells were stimulated with anti-CD3 and anti-CD28 plate-bound Abs, and with the indicated concentrations of dopamine. *A*, ELISA for IFN-γ, IL-5, and IL-17 was performed on the supernatants after a 3-d culture period. *B*, Cytokine beads array for IL-1β and IL-6 was performed on the supernatants after a 3-d culture period. *C*, Real-time PCR analysis of the expression of *rorc* transcript after stimulation. mRNA values were normalized to 18s. Purified human $CD4^+$ naive T cells were pretreated with 200 μg/ml tocilizumab or γ-globulin (as a control Ab) for 30 min and stimulated with 50 ng/ml PMA and 1 μg/ml ionomycin (*D*). PBS served as a negative control. Data are mean ± SD of five experiments in triplicate. Statistically significant differences are indicated by asterisks. $^{**}p < 0.01$, $^{*}p < 0.05$ versus control. Figures represent three independent experiments.

dopamine without anti-CD3/CD28 Abs. However, all cytokines that we tested were undetectable or very low level (data not shown). Furthermore, we investigated the *rorc* mRNA expression in these cells after stimulation with dopamine by quantitative PCR (Fig. 1*C*). Stimulation with anti-CD3/CD28 Abs induced the *rorc* mRNA expression, whereas dopamine markedly increased the expression level at 72 h. The induction of IL-17 secretion, which was dopamine dependent, was almost completely inhibited when human $CD4^+$ naive T cells were pretreated with tocilizumab, an anti-human IL-6R Ab (Fig. 1*D*). These results suggested that dopamine increases IL-17 production from T cells via IL-6 production.

D1-like receptor antagonists inhibit dopamine-mediated IL-6 and IL-17 secretion from human T cells

The IL-6 gene promoter contains a cAMP response element (46). In our previous studies, we showed that dopamine-mediated cAMP elevation in human $CD4^+$ naive T cells was completely inhibited by treatment with SCH-23390, a selective D1-like antagonist (41). To evaluate whether antagonizing D1-like receptors decreases dopamine-mediated IL-6 and IL-17 production, we treated $CD4^+$ naive T cells with or without SCH-23390, and then IL-6 and IL-17 secretion was determined by ELISA. As shown in Fig. 2, SCH-23390 completely inhibited dopamine-mediated IL-6 and IL-17 secretion from T cells. This inhibitory effect by antagonizing D1-like receptors was demonstrated not only by SCH-23390, but by LE300, another D1-like receptor antagonist (data not shown), indicating that antagonizing D1-like receptor inhibited dopamine-mediated IL-6–Th17 axis.

Dopamine is detected in inflamed synovial tissue in RA

To investigate the roles of dopamine in the pathogenesis of synovitis in RA, we measured catecholamine concentrations in synovial fluid of RA and OA patients (Table I). Although it is necessary to compare RA synovial tissue with synovial tissue from healthy individuals, we could not obtain samples from healthy individuals. Concentrations of noradrenalin and adrenaline did not differ between RA and OA patients, but dopamine was significantly higher in RA patients (Fig. 3*A*). Presumably, dopamine-producing cells were increased at the site of synovitis in RA. In the synovial tissues from RA patients, S100-positive DCs were also stained with dopamine, and an accumulation of lymphocytes

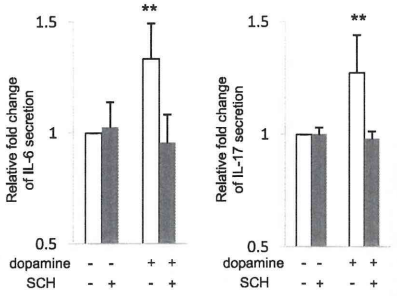

FIGURE 2. Suppression of dopamine-mediated upregulation of IL-6 and IL-17 production by a D1-like dopamine receptor antagonist. Purified human $CD4^+$ naive T cells were stimulated with anti-CD3 and anti-CD28 plate-bound Abs, 1 μM dopamine, and with or without 10 μM SCH-23390. White and gray bars represent without and with SCH-23390 exposure, respectively. Results are shown as relative fold changes compared with control cytokine production (not exposed to dopamine and SCH-23390). Data are mean ± SD of five experiments in triplicate. Statistically significant differences are indicated by asterisks. $^{**}p < 0.01$ versus control.

Table I. Clinical features of the participants who contributed synovial fluid

Characteristics	RA	OA
No. of participants	10	10
Sex, male/female	1/9	2/8
Mean age, y (range)	65.2 (39–85)	69.5 (57–78)
Mean disease duration, y (range)	5.2 (0.6–15)	NA
Mean CRP, mg/dl (range)	2.8 (1.5–4.4)	NA
Mean MMP3, ng/ml (range)	441.6 (135–738)	NA

CRP, C-reactive protein; MMP3, matrix metalloproteinase-3; NA, not applicable.

was prominently observed in the surroundings of DCs (Fig. 3*B*, 3*C*). Thus, it seems likely that there are DCs that synthesized and stored dopamine in RA synovial tissue.

Dopamine receptor antagonists on rheumatoid synovitis in SCID mice engrafted with human RA synovium mice

Next, to evaluate the relevance of these findings in vivo, we studied the effect of dopamine receptor antagonists in a model of the SCID mouse in which active RA synovial tissue and cartilage have been engrafted (SCID mice engrafted with human RA synovium [SCID-HuRAg]) (47). SCID-HuRAg mice were divided into three groups ($n = 6$) 1 wk after the transplantation, and an antagonist of D1-like receptors (SCH-23390), an antagonist of D2-like receptors (haloperidol), or vehicle (control) was administered twice a week for 3 wk for each group. The grafts were collected 30 d after implantation and pathological evaluation was performed. Macroscopically, remarkable retraction of synovial tissue was observed in the group that received D1-like receptor antagonist. In contrast, vascular proliferation and enlargement of tissue were observed in the group administered with D2-like receptor antagonist (Fig. 4*A*). The histopathological findings showed only slight

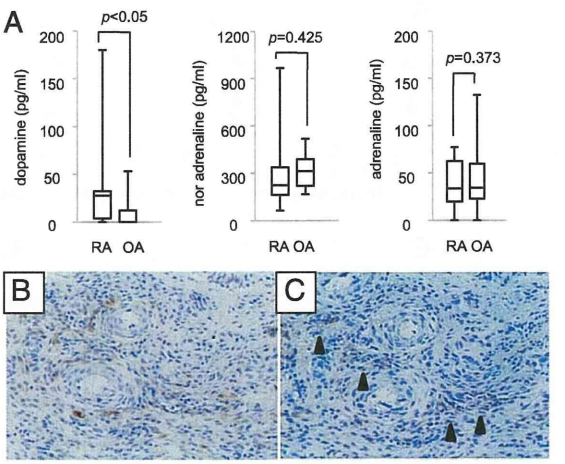

FIGURE 3. Presence of catecholamine in synovial fluids and the storage of dopamine in synovial tissue. *A*, Synovial fluids obtained from 10 patients with RA and 10 patients with OA were analyzed by HPLC electrochemical detection for dopamine, noradrenaline, and adrenaline. The composite results are presented as box plots, where the boxes represent the 25th to 75th percentiles, the lines within the boxes represent the median, and the lines outside the boxes represent the 10th to 90th percentiles. *B* and *C*, Immunohistochemical staining of S-100 protein (*B*) and dopamine (*C*) in RA synovial tissue (brown staining). Arrowheads indicate dopamine-stored cells (original magnification ×20). Sections are representative for three patients.

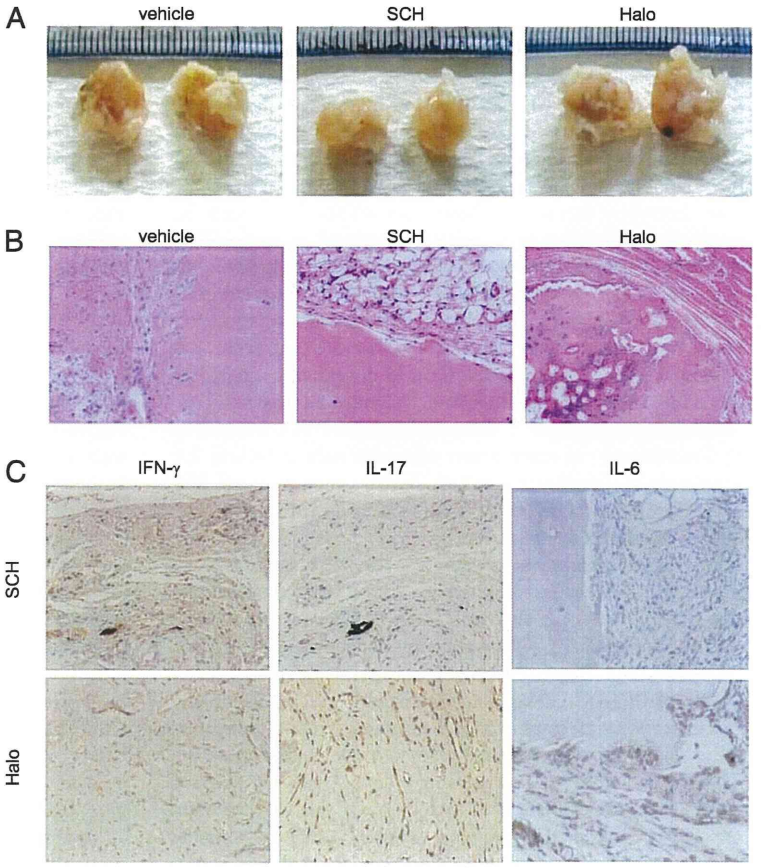

FIGURE 4. Differential effects of dopamine D1- and D2-like antagonists on experimental arthritis. *A*, The removed tissues containing synovium and cartilage from SCID-HuRAg mice. *B*, H&E-stained sections 30 d after implantation (original magnification ×20). *C*, IFN-γ and IL-6 are observed on brown staining. IL-17 is observed on pink staining. SCH23390-treated mice (*top panels*). Haloperidol-treated mice (*bottom panels*) (original magnification ×20). Sections are representative for $n \geq 3$ per group.

cartilage destruction, shrinkage of synovial fibroblasts, and prominent IFN-γ–producing cells in the group administered with D1-like receptor antagonist (Fig. 4*B*, 4*C*). In contrast, the group administered with D2-like receptor antagonist had marked cartilage destruction, synovial hyperplasia with angiogenesis, and prominent IL-6^+ and IL-17^+ cells (Fig. 4*B*, 4*C*). The effect of antagonizing D1-like receptor antagonist was demonstrated not only by SCH-23390, but by LE300, which is a selective D1-like receptor antagonist (data not shown).

D1-like receptor antagonists do not influence the viability of RA synovial fibroblasts

To clarify whether the retraction of synovial tissue in SCID-HuRAg mice treated with D1-like receptor antagonists is due to direct effect on synovial fibroblasts, we evaluated cell viability of SCH-23390–treated synovial fibroblasts using a WST-8 assay.

No significant differences were observed between antagonist-treated and untreated groups (Fig. 5*A*). Furthermore, we investigated the expression of dopamine receptors on synovial fibroblasts derived from RA patients. However, no D1–D5 subtype was detected on synovial fibroblasts (Fig. 5*B*). These results indicated that antagonizing D1-like receptors did not reduce synovial tissue in SCID-HuRAg mice directly.

Discussion

Dopamine has been shown to act on receptors present on immune cells, with all subtypes of dopamine receptors found on leukocytes (7, 8, 10). Interestingly, disorders such as schizophrenia and Parkinson's disease, in which there are changes in dopamine receptors and dopamine signaling pathways not only in brain, but in lymphocytes, are also associated with altered immune functioning (48). For example, in patients with schizophrenia thought to be

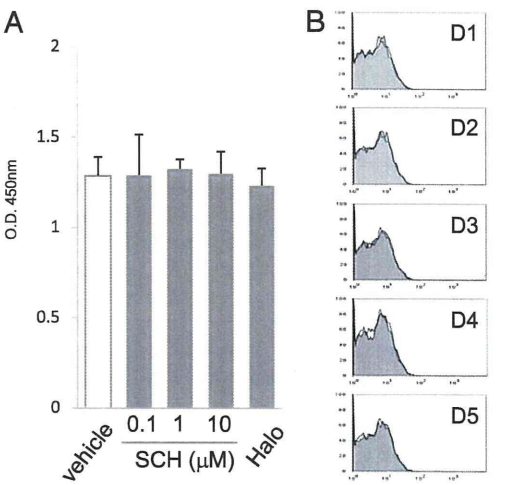

FIGURE 5. *A*, Effects of dopamine receptor antagonists on viability of synovial fibroblasts. Synovial fibroblasts were incubated with the indicated concentrations of SCH-23390 or 1 μM haloperidol for 24 h. Data are mean ± SD of five experiments in triplicate. *B*, The expression of dopamine receptor subtypes. The expression of dopamine receptor subtypes on human synovial fibroblasts was analyzed by a FACSCalibur. After fixation, cells were stained with Abs of indicated dopamine receptor subtypes and anti-rabbit IgG-FITC. Filled histograms indicate dopamine receptor subtypes; open histograms indicate isotype-matched control IgG. The results are representative of three experiments.

dependent on excessive response of D2-like dopamine receptors (49), the median incidence rate of RA is ~0.09% (50). This incidence is only one tenth that of RA in the general population, suggesting the involvement of dopamine signaling pathway in the pathogenesis of RA. However, there was no clear explanation for this epidemiological phenomenon.

The secondary lymphoid tissues are highly innervated by sympathetic nerve fibers that store high levels of dopamine (51), and lymphocytes also produce dopamine (52, 53). However, although RA synovium has been known to have the characteristics of lymphoid organs with regard to cellular composition and organization, a drastic loss of sympathetic nerve fibers in the RA synovium has been demonstrated (54). In our previous study, we demonstrated that monocyte-derived DC released vesicles containing dopamine toward T cells during DC–T cell interaction (41). Furthermore, we could detect dopamine only in DCs in RA synovium in our current study. These findings suggested that DC-derived dopamine during naive T cell–DC interaction may contribute to the development of RA.

During the development of RA, $CD45RA^+$ T cells may be attracted by chemokines secreted by tissue macrophages/DCs. Naive $CD45RA^+$ T cells expressing ICAM-3, which is a specific ligand of DC-specific ICAM-3–grabbing nonintegrin (DC-SIGN), are abundantly present within the RA synovium (55), suggesting that naive T cell–DC interaction is involved in cell activation and increased release of cytokines and enzymes. Although we had tried to characterize the phenotype of the putative DCs storing significant amounts of dopamine using several Abs to DC markers such as CD1a, CD123, and BDCA-2, these DC markers were not detectable by immunohistochemical staining, which is probably due to reduced antigenicity by fixation synovial membrane samples by 5% glutaraldehyde.

Although the concentration of dopamine in the RA synovial fluid was 0.1–10 nM, calculated dopamine concentration within 1 ms after unitary synaptic release was 100–250 nM within 1 μm in dopaminergic neurons (1). Because the space at DC–T cell synapses is within 1 μm (41), the concentration of dopamine in the synapse is estimated to be 100–250 nM, thus indicating that $CD4^+$ naive T cells might be exposed to a relatively high concentration of dopamine during DC–T cell interaction. The concentration of the dopamine we used was high compared with previous reports. However, when naive CD4 T cells were stimulated with both anti-CD3/CD28 mAb and dopamine, cell viability was not affected by dopamine up to 10 μM (data not shown). Previous in vitro studies testing dopamine at relatively high concentrations demonstrated that dopamine was immunosuppressive (14, 15). In contrast, in vivo administration of pharmacological doses of dopamine was reported to be mostly immunostimulatory (56). Thus, dopamine could be either immunostimulatory or immunosuppressive depending on the experimental condition used. However, it is highly possible that these findings are dependent on the expression pattern and the level of dopamine receptors.

Studies carried out on human and murine T cells have demonstrated that these cells express all subtypes of dopamine receptors, each of which has diverse modulatory effects on the T cell physiology. D1- and D2-like dopamine receptors are coupled to stimulation and inhibition of intracellular cAMP production, respectively (2, 13). Stimulation of the D1-like receptor impairs T cell function by increasing intracellular cAMP levels. Stimulation of D1-like receptor not only inhibits cytotoxic function of $CD8^+$ T cells (57), but impairs function and differentiation of regulatory T cells (Tregs) (53, 58). Stimulation of dopamine D2-like receptors in normal resting peripheral human T lymphocytes induces integrin-mediated adhesion to fibronectin (4) and increases the secretion of TNF-α (primarily via D3 receptors) and the secretion of IL-10 (primarily via D2 receptors) without affecting the secretion of IFN-γ and IL-4 (7). However, because these normal resting peripheral human T lymphocytes were not purified, they were different in quality from $CD4^+CD45RA^+$ naive T cells, which we used in this study. We have already reported that there were differences in the expression pattern of dopamine receptor subtypes between naive CD4 T cells and memory CD4 T cells (19), and that dopamine increases intracellular cAMP levels in naive CD4 T cells but decreases them in memory CD4 T cells (41). Therefore, high purity of $CD4^+CD45RA^+$ naive T cells was needed to reproduce the series of our results.

We have previously demonstrated that D1-like receptors were functionally dominant, and that dopamine increased cAMP levels via D1-like receptors and induced the production of Th2 cytokine such as IL-4 and IL-5, in response to anti-CD3/CD28 mAb (41). Regarding regulation of TCR-triggered signaling by cAMP in T cells, protein kinase A (a protein kinase activated by cAMP) and cAMP induce inhibition of ERK phosphorylation (59) and of JNK activation (60), activate C-terminal Src kinase (61), and block NF-κB activation (62, 63). All of these intracellular biochemical events induce a marked impairment on T cell activation with inhibition of T cell proliferation and of cytokine production (64). In this study, we showed that dopamine markedly increased IL-17 production from T cells via IL-6 production, in response to anti-CD3/CD28 mAb. Because the IL-6 gene promoter contains a cAMP response element (46), it is likely that increased intracellular cAMP via D1-like receptors of T cells induces IL-6 production, which act as autocrine or paracrine stimulus for IL-17 production in short-term culture. Although murine Th17 cells originate from $CD4^+$ naive T cells in the presence of IL-6 and TGF-β, the precise conditions for human Th17 differentiation remain controversial (65). Therefore, further studies are needed to elucidate the potential role of dopamine in human Th17 differentiation by long-term culture in the presence of TGF-β. However, in a human RA/SCID mouse chimera model, antagonizing dopamine receptor subtypes differentially affected cytokine expression, indicating that dopamine produced by DCs that accumulated in synovial tissue of RA established a Th17-predominant immune system via IL-6 and IL-17 production from T cells, leading to aggravation of synovitis and cartilage destruction.

Interestingly, it has been reported that dopamine reduces the suppressive and trafficking activities of naturally occurring Treg through D1-like receptors in both human and mouse (53, 58), and that dopamine-mediated downregulation of naturally occurring Tregs was selectively reversed by treatment with SCH-23390 (53, 58), indicating that DC-derived dopamine causes prolongation of RA synovitis via inhibition of Treg, as well as IL-6–Th17 bias. In other words, application of a D1-like receptor antagonist can be expected to control autoimmune disorders such as RA via two mechanisms: inhibition of IL-6–Th17 bias and increase in Treg activity. Actually, D1-like receptor antagonists exhibited preventive and therapeutic effects on model mice of autoimmune diseases such as EAE in mice, diabetes mellitus that occurs naturally in NOD mice, and crescent formation in nephrotoxic serum nephritis mice (19, 66, 67).

In this study, the specific importance of neuroimmune cross talk during pathological processes of various immune-inflammatory diseases was indicated, to our knowledge, for the first time by the discovery of dopamine production in DCs, which are the immunological sentinels at the front line of tissue defense and subsequent induction of Th17-predominant immune disease. In addition, approach from a different perspective could lead to new treatment applications of these findings.

Acknowledgments

We thank N. Sakaguchi, K. Noda, T. Adachi, and S. Shinohara for technical assistance.

Disclosures

Y.T. has received consulting fees, speaking fees, and/or honoraria from Mitsubishi Tanabe Pharma; Chugai Pharmaceutical Co., Ltd.; Eisai Co., Ltd.; Takeda Pharmaceutical Co., Ltd.; and Abbott Japan and has received research grant support from Mitsubishi Tanabe Pharma; Takeda Pharmaceutical Co., Ltd.; MSD; Pfizer; Astellas Pharma; Chugai Pharmaceutical Co., Ltd.; Abbott Japan; and Eisai Co., Ltd.

References

1. Wickens, J. R., and G. W. Arbuthnott. 2005. Structural and functional interactions in the striatum at the receptor level. In *Handbook of Chemical Neuroanatomy.* S. B. Dunnet, M. Bentivoglio, A. Bjorklund, and T. Hokfelt, eds. Elsevier Science Publishing Co., Amsterdam, p. 199–236.
2. Missale, C., S. R. Nash, S. W. Robinson, M. Jaber, and M. G. Caron. 1998. Dopamine receptors: from structure to function. *Physiol. Rev.* 78: 189–225.
3. Ganor, Y., M. Besser, N. Ben-Zakay, T. Unger, and M. Levite. 2003. Human T cells express a functional ionotropic glutamate receptor GluR3, and glutamate by itself triggers integrin-mediated adhesion to laminin and fibronectin and chemotactic migration. *J. Immunol.* 170: 4362–4372.
4. Levite, M., Y. Chowers, Y. Ganor, M. Besser, R. Hershkovits, and L. Cahalon. 2001. Dopamine interacts directly with its D3 and D2 receptors on normal human T cells, and activates beta1 integrin function. *Eur. J. Immunol.* 31: 3504–3512.
5. Franco, R., R. Pacheco, C. Lluis, G. P. Ahern, and P. J. O'Connell. 2007. The emergence of neurotransmitters as immune modulators. *Trends Immunol.* 28: 400–407.
6. Pacheco, R., H. Oliva, J. M. Martinez-Navío, N. Climent, F. Ciruela, J. M. Gatell, T. Gallart, J. Mallol, C. Lluis, and R. Franco. 2006. Glutamate released by dendritic cells as a novel modulator of T cell activation. *J. Immunol.* 177: 6695–6704.
7. Besser, M. J., Y. Ganor, and M. Levite. 2005. Dopamine by itself activates either D2, D3 or D1/D5 dopaminergic receptors in normal human T-cells and triggers the selective secretion of either IL-10, TNFalpha or both. *J. Neuroimmunol.* 169: 161–171.
8. Saha, B., A. C. Mondal, S. Basu, and P. S. Dasgupta. 2001. Circulating dopamine level, in lung carcinoma patients, inhibits proliferation and cytotoxicity of CD4+ and CD8+ T cells by D1 dopamine receptors: an in vitro analysis. *Int. Immunopharmacol.* 1: 1363–1374.
9. Sarkar, C., S. Das, D. Chakroborty, U. R. Chowdhury, B. Basu, P. S. Dasgupta, and S. Basu. 2006. Cutting edge: stimulation of dopamine D4 receptors induce T cell quiescence by up-regulating Kruppel-like factor-2 expression through inhibition of ERK1/ERK2 phosphorylation. *J. Immunol.* 177: 7525–7529.
10. Watanabe, Y., T. Nakayama, D. Nagakubo, K. Hieshima, Z. Jin, F. Katou, K. Hashimoto, and O. Yoshie. 2006. Dopamine selectively induces migration and homing of naive CD8+ T cells via dopamine receptor D3. *J. Immunol.* 176: 848–856.
11. O'Connell, P. J., X. Wang, M. Leon-Ponte, C. Griffiths, S. C. Pingle, and G. P. Ahern. 2006. A novel form of immune signaling revealed by transmission of the inflammatory mediator serotonin between dendritic cells and T cells. *Blood* 107: 1010–1017.
12. Kawashima, K., and T. Fujii. 2003. The lymphocytic cholinergic system and its contribution to the regulation of immune activity. *Life Sci.* 74: 675–696.
13. Sibley, D. R., F. J. Monsma, Jr., and Y. Shen. 1993. Molecular neurobiology of dopaminergic receptors. *Int. Rev. Neurobiol.* 35: 391–415.
14. Ghosh, M. C., A. C. Mondal, S. Basu, S. Banerjee, J. Majumder, D. Bhattacharya, and P. S. Dasgupta. 2003. Dopamine inhibits cytokine release and expression of tyrosine kinases, Lck and Fyn in activated T cells. *Int. Immunopharmacol.* 3: 1019–1026.
15. Bergquist, J., E. Josefsson, A. Tarkowski, R. Ekman, and A. Ewing. 1997. Measurements of catecholamine-mediated apoptosis of immunocompetent cells by capillary electrophoresis. *Electrophoresis* 18: 1760–1766.
16. Takahashi, N., Y. Nagai, S. Ueno, Y. Saeki, and T. Yanagihara. 1992. Human peripheral blood lymphocytes express D5 dopamine receptor gene and transcribe the two pseudogenes. *FEBS Lett.* 314: 23–25.
17. Ricci, A., E. Bronzetti, F. Mignini, S. K. Tayebati, D. Zaccheo, and F. Amenta. 1999. Dopamine D1-like receptor subtypes in human peripheral blood lymphocytes. *J. Neuroimmunol.* 96: 234–240.
18. McKenna, F., P. J. McLaughlin, B. J. Lewis, G. C. Sibbring, J. A. Cummerson, D. Bowen-Jones, and R. J. Moots. 2002. Dopamine receptor expression on human T- and B-lymphocytes, monocytes, neutrophils, eosinophils and NK cells: a flow cytometric study. *J. Neuroimmunol.* 132: 34–40.
19. Nakano, K., T. Higashi, K. Hashimoto, R. Takagi, Y. Tanaka, and S. Matsushita. 2008. Antagonizing dopamine D1-like receptor inhibits Th17 cell differentiation: preventive and therapeutic effects on experimental autoimmune encephalomyelitis. *Biochem. Biophys. Res. Commun.* 373: 286–291.
20. Volpe, E., N. Servant, R. Zollinger, S. I. Bogiatzi, P. Hupé, E. Barillot, and V. Soumelis. 2008. A critical function for transforming growth factor-beta, interleukin 23 and proinflammatory cytokines in driving and modulating human T (H)-17 responses. *Nat. Immunol.* 9: 650–657.
21. Yang, L., D. E. Anderson, C. Baecher-Allan, W. D. Hastings, E. Bettelli, M. Oukka, V. K. Kuchroo, and D. A. Hafler. 2008. IL-21 and TGF-β are required for differentiation of human T(H)17 cells. *Nature* 454: 350–352.
22. Santarlasci, V., L. Maggi, M. Capone, F. Frosali, V. Querci, R. De Palma, F. Liotta, L. Cosmi, E. Maggi, S. Romagnani, and F. Annunziato. 2009. TGF-β indirectly favors the development of human Th17 cells by inhibiting Th1 cells. *Eur. J. Immunol.* 39: 207–215.
23. Cua, D. J., J. Sherlock, Y. Chen, C. A. Murphy, B. Joyce, B. Seymour, L. Lucian, W. To, S. Kwan, T. Churakova, et al. 2003. Interleukin-23 rather than interleukin-12 is the critical cytokine for autoimmune inflammation of the brain. *Nature* 421: 744–748.
24. Murphy, C. A., C. L. Langrish, Y. Chen, W. Blumenschein, T. McClanahan, R. A. Kastelein, J. D. Sedgwick, and D. J. Cua. 2003. Divergent pro- and antiinflammatory roles for IL-23 and IL-12 in joint autoimmune inflammation. *J. Exp. Med.* 198: 1951–1957.
25. Kotake, S., N. Udagawa, N. Takahashi, K. Matsuzaki, K. Itoh, S. Ishiyama, S. Saito, K. Inoue, N. Kamatani, M. T. Gillespie, et al. 1999. IL-17 in synovial fluids from patients with rheumatoid arthritis is a potent stimulator of osteoclastogenesis. *J. Clin. Invest.* 103: 1345–1352.
26. Chabaud, M., J. M. Durand, N. Buchs, F. Fossiez, G. Page, L. Frappart, and P. Miossec. 1999. Human interleukin-17: a T cell-derived proinflammatory cytokine produced by the rheumatoid synovium. *Arthritis Rheum.* 42: 963–970.
27. Ziolkowska, M., A. Koc, G. Luszczykiewicz, K. Ksiezopolska-Pietrzak, E. Klimczak, H. Chwalinska-Sadowska, and W. Maslinski. 2000. High levels of IL-17 in rheumatoid arthritis patients: IL-15 triggers in vitro IL-17 production via cyclosporin A-sensitive mechanism. *J. Immunol.* 164: 2832–2838.
28. Honorati, M. C., R. Meliconi, L. Pulsatelli, S. Canè, L. Frizziero, and A. Facchini. 2001. High in vivo expression of interleukin-17 receptor in synovial endothelial cells and chondrocytes from arthritis patients. *Rheumatology (Oxford)* 40: 522–527.
29. Kirkham, B. W., M. N. Lassere, J. P. Edmonds, K. M. Juhasz, P. A. Bird, C. S. Lee, R. Shnier, and I. J. Portek. 2006. Synovial membrane cytokine expression is predictive of joint damage progression in rheumatoid arthritis: a two-year prospective study (the DAMAGE study cohort). *Arthritis Rheum.* 54: 1122–1131.
30. Chabaud, M., F. Fossiez, J.-L. Taupin, and P. Miossec. 1998. Enhancing effect of IL-17 on IL-1-induced IL-6 and leukemia inhibitory factor production by rheumatoid arthritis synoviocytes and its regulation by Th2 cytokines. *J. Immunol.* 161: 409–414.
31. Chabaud, M., G. Page, and P. Miossec. 2001. Enhancing effect of IL-1, IL-17, and TNF-α on macrophage inflammatory protein-3α production in rheumatoid arthritis: regulation by soluble receptors and Th2 cytokines. *J. Immunol.* 167: 6015–6020.
32. Katz, Y., O. Nadiv, and Y. Beer. 2001. Interleukin-17 enhances tumor necrosis factor alpha-induced synthesis of interleukins 1,6, and 8 in skin and synovial fibroblasts: a possible role as a "fine-tuning cytokine" in inflammation processes. *Arthritis Rheum.* 44: 2176–2184.
33. Lundy, S. K., S. Sarkar, L. A. Tesmer, and D. A. Fox. 2007. Cells of the synovium in rheumatoid arthritis. T lymphocytes. *Arthritis Res. Ther.* 9: 202.
34. Gaffen, S. L. 2004. Biology of recently discovered cytokines: interleukin-17—a unique inflammatory cytokine with roles in bone biology and arthritis. *Arthritis Res. Ther.* 6: 240–247.
35. Miranda-Carús, M. E., M. Benito-Miguel, A. Balsa, T. Cobo-Ibáñez, C. Pérez de Ayala, D. Pascual-Salcedo, and E. Martín-Mola. 2006. Peripheral blood T lymphocytes from patients with early rheumatoid arthritis express RANKL and interleukin-15 on the cell surface and promote osteoclastogenesis in autologous monocytes. *Arthritis Rheum.* 54: 1151–1164.
36. Sato, K., A. Suematsu, K. Okamoto, A. Yamaguchi, Y. Morishita, Y. Kadono, S. Tanaka, T. Kodama, S. Akira, Y. Iwakura, et al. 2006. Th17 functions as an osteoclastogenic helper T cell subset that links T cell activation and bone destruction. *J. Exp. Med.* 203: 2673–2682.
37. Koenders, M. I., E. Lubberts, F. A. J. van de Loo, B. Oppers-Walgreen, L. van den Bersselaar, M. M. Helsen, J. K. Kolls, F. E. Di Padova, L. A. B. Joosten, and W. B. van den Berg. 2006. Interleukin-17 acts independently of TNF-α under arthritic conditions. *J. Immunol.* 176: 6262–6269.
38. Koenders, M. I., J. K. Kolls, B. Oppers-Walgreen, L. van den Bersselaar, L. A. B. Joosten, J. R. Schurr, P. Schwarzenberger, W. B. van den Berg, and E. Lubberts. 2005. Interleukin-17 receptor deficiency results in impaired synovial expression of interleukin-1 and matrix metalloproteinases 3, 9, and 13 and prevents cartilage destruction during chronic reactivated streptococcal cell wall-induced arthritis. *Arthritis Rheum.* 52: 3239–3247.
39. Genovese, M. C., F. Van den Bosch, S. A. Roberson, S. Bojin, I. M. Biagini, P. Ryan, and J. Sloan-Lancaster. 2010. LY2439821, a humanized anti-interleukin-17 monoclonal antibody, in the treatment of patients with rheumatoid arthritis: a phase I randomized, double-blind, placebo-controlled, proof-of-concept study. *Arthritis Rheum.* 62: 929–939.
40. M rphy, K. M., W. Ouyang, J. D. Farrar, J. Yang, S. Ranganath, H. Asnagli, M. Afkarian, and T. L. Murphy. 2000. Signaling and transcription in T helper development. *Annu. Rev. Immunol.* 18: 451–494.
41. Nakano, K., T. Higashi, R. Takagi, K. Hashimoto, Y. Tanaka, and S. Matsushita. 2009. Dopamine released by dendritic cells polarizes Th2 differentiation. *Int. Immunol.* 21: 645–654.
42. Arnett, F. C., S. M. Edworthy, D. A. Bloch, D. J. McShane, J. F. Fries, N. S. Cooper, L. A. Healey, S. R. Kaplan, M. H. Liang, H. S. Luthra, et al. 1988.

The American Rheumatism Association 1987 revised criteria for the classification of rheumatoid arthritis. *Arthritis Rheum.* 31: 315–324.
43. Yanagihara, N., Y. Oishi, H. Yamamoto, M. Tsutsui, J. Kondoh, T. Sugiura, E. Miyamoto, and F. Izumi. 1996. Phosphorylation of chromogranin A and catecholamine secretion stimulated by elevation of intracellular Ca2+ in cultured bovine adrenal medullary cells. *J. Biol. Chem.* 271: 17463–17468.
44. Sasaguri, Y., K.-Y. Wang, A. Tanimoto, M. Tsutsui, H. Ueno, Y. Murata, Y. Kohno, S. Yamada, and H. Ohtsu. 2005. Role of histamine produced by bone marrow-derived vascular cells in pathogenesis of atherosclerosis. *Circ. Res.* 96: 974–981.
45. Nakano, K., Y. Okada, K. Saito, R. Tanikawa, N. Sawamukai, Y. Sasaguri, T. Kohro, Y. Wada, T. Kodama, and Y. Tanaka. 2007. Rheumatoid synovial endothelial cells produce macrophage colony-stimulating factor leading to osteoclastogenesis in rheumatoid arthritis. *Rheumatology (Oxford)* 46: 597–603.
46. Sitaraman, S. V., D. Merlin, L. Wang, M. Wong, A. T. Gewirtz, M. Si-Tahar, and J. L. Madara. 2001. Neutrophil-epithelial crosstalk at the intestinal lumenal surface mediated by reciprocal secretion of adenosine and IL-6. *J. Clin. Invest.* 107: 861–869.
47. Geiler, T., J. Kriegsmann, G. M. Keyszer, R. E. Gay, and S. Gay. 1994. A new model for rheumatoid arthritis generated by engraftment of rheumatoid synovial tissue and normal human cartilage into SCID mice. *Arthritis Rheum.* 37: 1664–1671.
48. Sarkar, C., B. Basu, D. Chakroborty, P. S. Dasgupta, and S. Basu. 2010. The immunoregulatory role of dopamine: an update. *Brain Behav. Immun.* 24: 525–528.
49. Abi-Dargham, A., J. Rodenhiser, D. Printz, Y. Zea-Ponce, R. Gil, L. S. Kegeles, R. Weiss, T. B. Cooper, J. J. Mann, R. L. Van Heertum, et al. 2000. Increased baseline occupancy of D2 receptors by dopamine in schizophrenia. *Proc. Natl. Acad. Sci. USA* 97: 8104–8109.
50. Oken, R. J., and M. Schulzer. 1999. At issue: schizophrenia and rheumatoid arthritis: the negative association revisited. *Schizophr. Bull.* 25: 625–638.
51. Weihe, E., D. Nohr, S. Michel, S. Müller, H. J. Zentel, T. Fink, and J. Krekel. 1991. Molecular anatomy of the neuro-immune connection. *Int. J. Neurosci.* 59: 1–23.
52. Bergquist, J., A. Tarkowski, R. Ekman, and A. Ewing. 1994. Discovery of endogenous catecholamines in lymphocytes and evidence for catecholamine regulation of lymphocyte function via an autocrine loop. *Proc. Natl. Acad. Sci. USA* 91: 12912–12916.
53. Cosentino, M., A. M. Fietta, M. Ferrari, E. Rasini, R. Bombelli, E. Carcano, F. Saporiti, F. Meloni, F. Marino, and S. Lecchini. 2007. Human CD4+CD25+ regulatory T cells selectively express tyrosine hydroxylase and contain endogenous catecholamines subserving an autocrine/paracrine inhibitory functional loop. *Blood* 109: 632–642.
54. Capellino, S., M. Cosentino, C. Wolff, M. Schmidt, J. Grifka, and R. H. Straub. 2010. Catecholamine-producing cells in the synovial tissue during arthritis: modulation of sympathetic neurotransmitters as new therapeutic target. *Ann. Rheum. Dis.* 69: 1853–1860.
55. van Lent, P. L., C. G. Figdor, P. Barrera, K. van Ginkel, A. Slöetjes, W. B. van den Berg, and R. Torensma. 2003. Expression of the dendritic cell-associated C-type lectin DC-SIGN by inflammatory matrix metalloproteinase-producing macrophages in rheumatoid arthritis synovium and interaction with intercellular adhesion molecule 3-positive T cells. *Arthritis Rheum.* 48: 360–369.
56. Basu, S., and P. S. Dasgupta. 2000. Dopamine, a neurotransmitter, influences the immune system. *J. Neuroimmunol.* 102: 113–124.
57. Saha, B., A. C. Mondal, J. Majumder, S. Basu, and P. S. Dasgupta. 2001. Physiological concentrations of dopamine inhibit the proliferation and cytotoxicity of human CD4+ and CD8+ T cells in vitro: a receptor-mediated mechanism. *Neuroimmunomodulation* 9: 23–33.
58. Kipnis, J., M. Cardon, H. Avidan, G. M. Lewitus, S. Mordechay, A. Rolls, Y. Shani, and M. Schwartz. 2004. Dopamine, through the extracellular signal-regulated kinase pathway, downregulates CD4+CD25+ regulatory T-cell activity: implications for neurodegeneration. *J. Neurosci.* 24: 6133–6143.
59. Ramstad, C., V. Sundvold, H. K. Johansen, and T. Lea. 2000. cAMP-dependent protein kinase (PKA) inhibits T cell activation by phosphorylating ser-43 of raf-1 in the MAPK/ERK pathway. *Cell. Signal.* 12: 557–563.
60. Harada, Y., S. Miyatake, K.-i. Arai, and S. Watanabe. 1999. Cyclic AMP inhibits the activity of JNK (JNKp46) but not JNKp55 and ERK2 in human helper T lymphocytes. *Biochem. Biophys. Res. Commun.* 266: 129–134.
61. Vang, T., K. M. Torgersen, V. Sundvold, M. Saxena, F. O. Levy, B. S. Skålhegg, V. Hansson, T. Mustelin, and K. Taskén. 2001. Activation of the COOH-terminal Src kinase (Csk) by cAMP-dependent protein kinase inhibits signaling through the T cell receptor. *J. Exp. Med.* 193: 497–507.
62. Hershfield, M. S. 2005. New insights into adenosine-receptor-mediated immunosuppression and the role of adenosine in causing the immunodeficiency associated with adenosine deaminase deficiency. *Eur. J. Immunol.* 35: 25–30.
63. Jimenez, J. L., C. Punzón, J. Navarro, M. A. Muñoz-Fernández, and M. Fresno. 2001. Phosphodiesterase 4 inhibitors prevent cytokine secretion by T lymphocytes by inhibiting nuclear factor-kappaB and nuclear factor of activated T cells activation. *J. Pharmacol. Exp. Ther.* 299: 753–759.
64. Aandahl, E. M., W. J. Moretto, P. A. Haslett, T. Vang, T. Bryn, K. Tasken, and D. F. Nixon. 2002. Inhibition of antigen-specific T cell proliferation and cytokine production by protein kinase A type I. *J. Immunol.* 169: 802–808.
65. Korn, T., E. Bettelli, M. Oukka, and V. K. Kuchroo. 2009. IL-17 and Th17 Cells. *Annu. Rev. Immunol.* 27: 485–517.
66. Hashimoto, K., T. Inoue, T. Higashi, S.-i. Takei, T. Awata, S. Katayama, R. Takagi, H. Okada, and S. Matsushita. 2009. Dopamine D1-like receptor antagonist, SCH23390, exhibits a preventive effect on diabetes mellitus that occurs naturally in NOD mice. *Biochem. Biophys. Res. Commun.* 383: 460–463.
67. Okada, H., T. Inoue, K. Hashimoto, H. Suzuki, and S. Matsushita. 2009. D1-like receptor antagonist inhibits IL-17 expression and attenuates crescent formation in nephrotoxic serum nephritis. *Am. J. Nephrol.* 30: 274–279.

資　料

資料１．骨検診に用いた説明書・同意書等の写し

大府市

新しい骨検診法の性能試験参加のおねがい

レディースドック受検予定のみなさまへ

高齢者、とくに高齢女性の骨折が年々増加しています。とくに足の付け根の骨折件数は年間15万人にもなり、そのまま寝たきりになることも多いのです。原因のひとつに骨粗鬆症があります。国は骨折予防のための骨粗鬆症検診（骨検診）を推奨しておりますが、実際に検診を受けられる方はまだまだ少ないのが現状です。

私たちは、簡単に骨の状態をチェックができる新しい方法を開発しました。現在レディースドックを受検される方々を対象に、この方法の性能試験参加をお願いしておりますが、平成23年度も引き続き参加をお願いしております（昨年受けた方も継続して参加してください）

参加ご希望の方は、同封の試験の目的や方法についての説明書をよくお読みください。なお、検査に係る費用はいっさい発生いたしません。

試験に関する説明について十分ご理解頂き、参加にご同意頂けるときは、同封の同意書にご署名とご連絡先（結果の送付先）をご記入の上、レディースドック当日にご持参ください。**（すでに同意書を提出頂いている方は不要です。）**

ご協力、よろしくお願いいたします。

厚生労働省長寿科学総合研究事業
研究班代表
国立長寿医療研究センター　新飯田俊平

様式１－２

大府市

骨粗鬆症の新しい検査法の性能試験について

わが国の骨粗鬆症検診（骨検診）の受診率は非常に低いのが現状です。少しでも多くの方々に骨検診を受けてもらうため、私たちは低コストで簡便な骨検診法を開発しました。しかし、この検査方法を実用化するためには、実際の骨検診でどれくらいの効果を発揮するかを検証する必要があります。以下に、今回の性能試験の目的と、研究対象者や方法について説明いたします。

１．試験の目的

この検査方法で、骨量減少症または骨粗鬆症の人をどれくらいの精度で見つけることが出来るかを評価することが目的です。

２．検査対象者の抽出と対象年齢

- 大府市のレディースドックの申込者を対象とさせて頂いております。
- 本年度の尿検診は **40 歳以上**とさせて頂きます（39 歳以下でもご希望があれば当日尿をご持参ください）

３．どんな検査をするのか

尿中に存在する、γ－グルタミルトランスペプチダーゼ（γ-GTP）という酵素の活性値を測定します。この値が高いほど骨吸収が亢進（骨が減る）している状態にあると考えられます。

４．試験の方法

- 検査は**検査当日の早朝の尿**を用いて測定します。 **起床後に同封の採尿キットで尿をびんの線のある位置まで**入れて検診会場にお持ちください。
- この検査方法を評価するために、同じ尿を使っての既存の骨代謝マーカーを一緒に測定する場合があります。
- 骨折リスク判定のための**問診票（同封の白い紙）の記入**をお願いします。

５．結果の通知方法

検査結果は本人に直接封書にて通知いたします。**骨吸収が亢進状態**にある方にはその後の医療機関受診の有無などを調査するために電話等で確認させて頂くことがありますのでご協力をお願い致します。

６．健康上の被害と補償について

採尿したものを使用させていただくだけですので健康を害するものではありません。骨密度測定では、微量の X 線に被爆しますが、胸のレントゲンの 1/15 程度ですので、健康を害するものではありません。

７．個人情報の保護について

この試験で得られた結果は、厚生労働省への提出資料として使用したり、医学会、医学雑誌などで発表することはありますが、参加者の名前などの個人情報は一切わからないようにいたしますので、プライバシーは完全に守られます。

裏面につづく

８．試験への参加と辞退について

この試験への参加は患者様の自由意志によるものです。また、いったん同意した後でも取り消すことはいつでもできますので、ご遠慮なく申し出てください。なお、この試験への協力を拒否したり、同意を取り消しても、検診上の不利益を受けることは一切ありません。

９．利益相反について

この研究に関わる全ての関係者は、本研究に関係するいかなる企業、団体からも金銭その他の利益の供与を受けていません。

10．試験の相談窓口について

この試験の内容など、何かわからないことや気になること、聞きたいことがありましたら、どのようなことでも遠慮なく下記の研究責任者におたずねください。

【研究責任者の所属・氏名】

国立長寿医療研究センター 遺伝子蛋白質解析室 室長　新飯田俊平

【連絡先】 電話 0562-46-2311（内線 5901）

【対象とする疾患名】 骨粗鬆症、骨量減少症